M-AM-SymI-1

CLASSES and FUNCTIONS of CALCIUM WAVES Lionel F. Jaffe, Marine Biological Laboratory, Woods Hole, MA 02543 [See Cell Calcium Nov. 1993 **14**, 736-745]

Fast calcium waves underlie most calcium signals. They are driven by a reaction-diffusion mechanism in which a rapid rise of cytosolic Ca^{2+} (in the 1 to 30 μM range) induces the release of Ca^{2+} from the lumen of the ER. This released Ca^{2+} then diffuses a short way through the cytosol to release more Ca^{2+} from the ER. Such waves are often begun by a second, lumenal mode of calcium induced calcium release begun by a slow rise of Ca^{2+} to millimolar trigger levels within the ER.

Fast wave functions go from the activation of eggs by sperm and the mediation of various hormonal messages to carrying various brain injury waves. In addition to carrying messages deep into cells and tissues, fast calcium waves may also act to transport fluid across epithelia.

M-AM-SymI-2

Molecular Basis of Fast Calcium Waves
Antony Galione, University Department of Pharmacology, Mansfield Road, Oxford OX1 3QT, UK

Regenerative Ca^{2+} waves are a prominent spatial feature of Ca^{2+} signals in many cell types. Intracellular Ca^{2+} waves are thought to occur by a regenerative release mechanism involving Ca^{2+}-induced Ca^{2+} release from intracellular stores. Two classes of structurally and functionally homologous Ca^{2+} release channel have been characterized on Ca^{2+} stores. The first is the inositol 1,4,5 trisphosphate receptor and the second is the ryanodine receptor. Evidence from studies using both intact cells and broken cell preparations suggest that both channel classes can give rise to Ca^{2+}-induced Ca^{2+} release. Furthermore, both classes of Ca^{2+} release channel can be gated by different intracellular signal molecules. While inositol 1,4,5 trisphosphate is a well characterized second messenger modulating inositol trisphosphate receptors, there is mounting evidence that cyclic ADP-ribose may regulate isoforms of ryanodine receptors, perhaps in an analogous way. In the sea urchin egg calcium waves initiated at fertilization can be propagated independently by both inositol trisphosphate and ryanodine receptors implying a redundancy of mechanism. Such redundancy may allow for modulation and diversity in the generation of Ca^{2+} waves.

M-AM-SymI-3

SLOW CALCIUM WAVES AND CYTOKINESIS. ((A.L. Miller))MBL, Woods Hole, MA 02543.

It has become apparent that there are three main classes of intracellular calcium waves: Ultrafast, Fast, and Slow, with velocities of 10^4-10^8, 5-30, and 0.1-1 μm/sec at 20° C respectively. The propagating mechanisms of the first two categories has been determined to be electrical fields and calcium-induced calcium release (CICR) respectively. A number of cogent arguments indicate that slow waves are not propagated by either of these mechanisms, rather they are propagated by mechanical forces generated within the cell. In the case of cytokinesis, it appears that the elongating and contracting furrow extends itself by tugging on cytoskeletal elemenents attached to stretch-sensitive channels in the ER and/or plasma membrane ahead of the advancing furrow. It is suggested that this mechanical release of calcium propagates the slow wave. Such a mechanical release could explain why furrowing waves (and the furrows themselves) extend in straight lines, whereas a diffusing propagator should spread out in all directions. Mechanical propagation also helps explain the slow velocity of these waves. They are about 100 times slower than fast waves. If propagated by CICR, the reaction rates would have to be the order of 10,000 times slower, a situation hard to imagine. We have demonstrated that mechanical deformation of Xenopus cell cycle extracts induces a reproducible calcium release that is rapidly resequestered by a functional ER.

M-AM-SymI-4

BRAIN INJURY WAVES. Stephen J. Smith, Dept. of Molecular and Cellular Physiology, Stanford University.

STRIATED MUSCLE PHYSIOLOGY AND ULTRASTRUCTURE I

M-AM-A1

Ca^{2+}-INDEPENDENT FORCE IN MAMMALIAN SKELETAL MUSCLE.
((G.J. Wilson[1], G.H. Rossmanith[2], S. Harroothunian[2] and J.F.Y. Hoh[3])) Departments of [1]Pathology and [3]Physiology, University of Sydney, NSW, 2006, Australia and [2]School of Mathematics, Physics, Computing & Electronics, Macquarie University, NSW, 2109, Australia.

Vanadate (Vi) extracts Troponin I (TnI) from mammalian cardiac muscle fibres, resulting in Ca^{2+}-independent force (Strauss *et al.*, 1992. FEBS Letters, **310**, 229). Using Vi we obtained Ca^{2+}-independent force in skinned mammalian skeletal muscle fibres incubated in Vi-relaxing or Vi-rigor ([Vi]=10mM, pH 7) solutions. Slow-twitch fibres exhibited Ca^{2+}-independent force after Vi-relaxing treatment, with some loss of Ca^{2+}-activated force. Ca^{2+}-activated force was reduced while no Ca^{2+}-independent force was observed in fast-twitch fibres incubated in Vi-relaxing solution. Vi is an oxidizing agent (oxidation state V^V) and could oxidize the myosin reactive sulphydryls (Wilson *et al.*, 1991. J.Physiol. **437**, 409), accounting for the decline in Ca^{2+}-activated force. If fast-twitch and slow-twitch fibres were subsequently treated with DTT, Ca^{2+}-activated force increased, implicating the sulphydryls in the Vi effect. Since the rigor state protects myosin sulphydryls from oxidizing agents (Wilson *et al.*, 1991), fibres in the rigor state were incubated in Vi. After Vi-rigor treatment fast-twitch fibres exhibited Ca^{2+}-independent force. Subsequent treatment with DTT did not further augment force, indicating that the myosin sulphydryls had been protected from Vi. Therefore Ca^{2+}-independent force was probably not seen after Vi-relaxing treatment of fast-twitch fibres because force generation was inhibited by myosin sulphydryl modification. Supported by ARC Australia, NH&MRC Australia and Faculty of Medicine, University of Sydney.

M-AM-A2

NITROPHENYL-EGTA, A NEW CAGED CA, WHICH SELECTIVELY BINDS CA WITH HIGH AFFINITY AND RELEASES IT RAPIDLY UPON PHOTOLYSIS
((Graham C.R. Ellis-Davies and Jack H. Kaplan)) Physiology Dept., University of Pennsylvania, Philadelphia, PA 19104-6085

Nitrophenyl-EGTA is a photosensitive derivative of EGTA which has a K_d for Ca^{2+} of 80 nM; upon illumination with uv light (300-400 nm) the chelator is bifurcated, yielding iminodiacetic acid photoproducts with low Ca affinity (K_d=1 mM). The change in K_d of 12 500-fold results in the photo-liberation of bound Ca^{2+}:

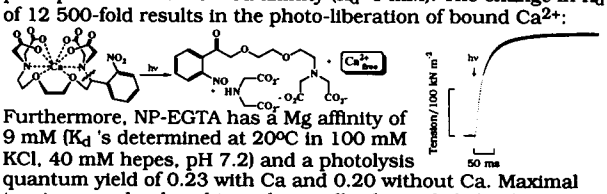

Furthermore, NP-EGTA has a Mg affinity of 9 mM (K_d 's determined at 20°C in 100 mM KCl, 40 mM hepes, pH 7.2) and a photolysis quantum yield of 0.23 with Ca and 0.20 without Ca. Maximal tension was developed in a chemically skinned skeletal muscle fibre with a half-time of 18 ms at 15°C and 1 mM $[Mg^{2+}]_{free}$ when Ca was photo-released from NP-EGTA. Therefore, NP-EGTA can be used for the rapid, selective and efficient release of Ca in the presence of physiological [Mg] in the study of intracellular Ca-dependent processes. Supported by NIH GM39500 and HL30315.

M-AM-A3

ACTIVATION OF SKINNED CARDIAC MUSCLE BY LASER PHOTOLYSIS OF NITROPHENYL-EGTA

((Robert J. Barsotti, Hunter Martin, Jack H. Kaplan,* and Graham C.R. Ellis-Davies*)) Bockus Research Inst. The Graduate Hospital, *Dept. of Physiology, University of Pennsylvania, Philadelphia, PA

Chemically skinned trabeculae of the guinea-pig were fully relaxed by incubation in a solution containing 2mM NP-EGTA, 1mM free Mg^{2+}, 5mM MgATP, and 20mM CP (pCa 6.0, I=200mM, pH 7.1, 21°C). Contractions were initiated by a laser pulse (λ =347nm, 50nsec, 140mJ) which photolyzed at least 10% of NP-EGTA and produced peak force. A brief delay of ~8ms was observed before the onset of isometric force. The time course of force was fit to a double exponential to study the dependence of its rate on the final $[Ca^{2+}]$, altered from pCa 6.0 to 4.8 by varying laser energy. The rates of both components of force development were Ca^{2+} sensitive and averaged 45 ± 5 and 8 ± 1 s^{-1} (mean ± sem, n=8) at $[Ca^{2+}]$ that induced peak force. By comparison, the rate of force development from rigor initiated by the photolytic release of ATP in Ca^{2+} (pCa 4.5) averaged only 18 ± 2 and 2 ± 0.3 s^{-1} (n=19). These results indicate that in cardiac muscle, 1) the rate of force development in contractions initiated from the relaxed state is sensitive to the $[Ca^{2+}]$, and 2) the rate of force development in contractions evoked from rigor may be limited by the ATP hydrolysis step of the cross-bridge cycle.

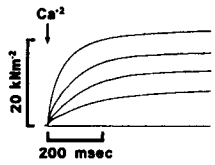

Supported By NIH HL40953 to R.J.B.; GM 39500 & HL30315 to J.H.K.

M-AM-A4

SINGLE CARDIAC MYOFIBRILS PRODUCE LESS ACTIVE FORCE THAN SINGLE SKELETAL MYOFIBRILS.

((W.A. Linke, V.I. Popov and G.H. Pollack)) Bioengineering WD-12, University of Washington, Seattle, WA 98195, USA.

We measured passive and active tension in single cardiac myofibrils. Experiments were performed using isolated myofibrils from chemically skinned rabbit heart, and employed a setup described previously (Bartoo *et al., J. Musc. Res. Cell Motil.*, in press; Fearn *et al., IEEE Trans. Biomed. Eng.*, in press; Linke *et al., Circ. Res.* 73:724-734, 1993).

Single myofibrils had an average slack sarcomere length (SL) in relaxing solution of 1.93 µm. Passive tension values were similar to values reported in larger specimens up to SL's of approximately 2.2 µm. Thus, at physiological SL's, the element responsible for most, if not all, passive force of cardiac muscle resides within the myofibrils. Above 2.2 µm, passive tension was considerably lower than that in larger preparations. Hence, the high resting tension at longer SL's in larger specimens is probably caused by non-myofibrillar structures. Resting tension at all lengths was not altered by the active-force-suppressing drug, BDM (10-100 mM), indicating that the myofibril-based passive force is unlikely to result from interactions between the contractile proteins; rather, it is very likely due to the presence and extensibility of the connecting filaments.

Maximum active isometric tension (pCa 5.0-4.5) at SL's of 2.1 to 2.3 µm averaged approximately 100 mN/mm². Compared with that in multicellular preparations, this value ranges slightly below values measured during sarcomere-isometric contractions, but is well above those reported in muscle-isometric contractions. However, it is considerably lower than the active tension value of approximately 600 mN/mm² measured in single skeletal myofibrils under similar conditions (Bartoo *et al., op. cit.*). The reason for this difference is not clear but may be due to the expression of different myosin isoforms in cardiac and skeletal muscle.

M-AM-A5

ALKALI LIGHT CHAIN COMPOSITION DETERMINES MAXIMUM SPEED OF SHORTENING, BUT NOT ATPase ACTIVITY IN FAST SKELETAL MUSCLE FIBRES OF THE RAT.

((R. Bottinelli, M. Canepari, C. Reggiani, G. Stienen*)) Inst. of Human Physiology, Univ. of Pavia, Italy and *Inst. for Cardiovascular Res., V.U., Amsterdam, The Netherlands. (spons. by G. Cecchi).

The proportion of the 3f isoform of alkali myosin might chain (MLC3f) has been shown to be a major determinant of maximum speed of shortening (Vo). Here we report that other kinetics parameters (isometric ATPase activity, and tension cost) are independent of MLC3f proportion. Vo, ATPase activity, tension cost (ATPase/tension) of chemically skinned fibres from tibialis anterior muscles of adult rats were determined. Fibres were maximally activated at 12° C and 2.7 µm sarcomere length. Vo was determined with the slack-test procedure in 5-6 subsequent activations. ATPase activity was studied in isometric conditions. ATPase assay was based on spectrophotometrical determination of NADH oxidation enzymatically coupled to ATP regeneration. All fibres were characterized as regards myosin heavy chain isoform composition (MHC) and alkali MLC isoform ratio by SDS-PAGE. For fibres containing 2B MHC and variable (from 26% to 57%) proportion of MLC3f, regression analysis of Vo, ATPase activity, ATPase/tension on MLC3f relative content was performed. Whereas Vo (range 2.11-5.47 L/s) highly correlated with the proportion of MLC3f, ATPase activity (mean ± S.E.M. 0.23±0.01 nmol Pi/mm³/s) and tension cost (2.89±0.09 pmol ATP/mN.mm.s) did not correlate. These results confirm that alkali MLC play a role of fine tuning shortening speed at low loads, but suggest that they are not involved in the regulation of ATP splitting rate and economy of force generation in isometric conditions. (Supported by Telethon n. 343).

M-AM-A6

EFFECTS OF pH ON MYOFIBRILLAR ATP TURNOVER IN FAST AND SLOW SKELETAL MUSCLE FIBERS OF THE RABBIT.

((E.J. Potma, I.A. van Graas and G.J.M. Stienen)) Laboratory for Physiology, Free University, v.d. Boechorststraat 7, 1081BT Amsterdam, the Netherlands.

The effect of pH on isometric myofibrillar ATPase activity and force was studied in the range from pH 6.4 to 7.9, in permeabilized single fibers of rabbit psoas and soleus muscle at 15°C, sarcomere length 2.4 µm and pCa 4.5. ATPase activity was measured photometrically by enzymatic coupling of the regeneration of ATP to the oxidation of NADH. NADH absorbance at 340 nm was determined in the measuring chamber. To measure ATP turnover in single soleus fibers accurately, a new measuring chamber (volume 4 µl) was developed which produced an approximately 8 times higher sensitivity than the system previously used. Under control conditions (pH 7.3), the isometric force was 136 kN/m² and 115 kN/m² and the ATPase activity was 0.43 mM/s and 0.055 mM/s, in psoas and soleus fibers respectively.

Isometric force increased monotonically with increasing pH. From pH 6.4 to 7.9 force increased by a factor 1.7 and 1.2 for psoas and soleus fibers, respectively. The isometric ATPase activity in psoas was constant over the entire pH range studied whereas in soleus it slightly decreased with increasing pH. These results indicate that the isometric tension cost and thus the apparent rate of crossbridge detachment decrease by a factor 0.56 as pH increases from 6.4 to 7.9, both for fast and slow skeletal muscle fibers.

M-AM-A7

FORCE AND SARCOMERE STIFFNESS KINETICS OF SKINNED SKELETAL MUSCLE FIBERS INHIBITED BY ALUMINOFLUORIDE.

((P.B. Chase, D.A. Martyn and J.D. Hannon)) Dept. of Radiology and Center for Bioengineering, University of Washington, Seattle, WA 98195, and Dept. of Anesthesiology, Mayo Clinic, Rochester, MN 55905

The mechanism of force inhibition by aluminofluoride (AlF), a slowly dissociating Pi analog, was examined in single, permeabilized fibers from rabbit psoas by measuring the Ca^{2+}-dependence of the kinetics of inhibitor dissociation and the kinetics of actomyosin interactions with AlF bound to the crossbridges. Kinetic properties of crossbridges attached to actin were characterized using ramp stretches (< 5 nm·h.s.$^{-1}$). Stiffness exhibited a steep dependence on the rate of stretch at maximum Ca^{2+}-activation (pCa 4.0, 0.2 M Γ/2). AlF inhibition at pCa 4.0 decreased stiffness at all speeds of stretch examined, with stiffness at high speeds (10^3 - 10^4 nm·h.s.$^{-1}$·s^{-1}) being disproportionately reduced. Relaxation of inhibited fibers (pCa 9.2, 0.2 M Γ/2) resulted in AlF being 'trapped' and was accompanied by further decrease in stiffness at all speeds to control relaxed values. At pCa 9.2 and 0.02 M Γ/2, which promotes weak crossbridge binding, stiffness at all rates of stretch was significantly inhibited by AlF 'trapped' in the fiber. To determine the Ca^{2+}-dependence of inhibitor dissociation, force was regulated independent of Ca^{2+} using an activating troponin C (aTnC). Results obtained with aTnC-activated fibers confirmed that there is no absolute requirement for Ca^{2+} for recovery from force inhibition by Pi analogs; the only requirement is thin filament activation which enables active crossbridge cycling. These results indicate that AlF preferentially inhibits rapid equilibrium or weak crossbridge attachment to actin, that AlF-bound crossbridges attach tightly to the activated thin filament, and that, at maximal (or near-maximal) activation, crossbridge attachment to actin prior to Pi analog dissociation is the primary event regulated by Ca^{2+}. Supported by NIH HL31962 and NS08384.

M-AM-A8

ACTIVE RAMP SHORTENING OF BUNDLES OF 1-3 MYOFIBRILS FROM RABBIT *PSOAS* MUSCLE

((A.L. Friedman and Y.E. Goldman)) Depts. of Bioengineering and Physiology, Univ. of Penna., Phila., PA 19104.

Active shortening in isolated myofibrils or small bundles is interesting because the individual sarcomeres can be directly observed during energy transduction. Following Iwazumi (*Am. J. Physiol.* 252:C253, 1987), we have built an instrument capable of applying programmed length changes and measuring the nano-Newton forces produced by myofibrils. The tissue is suspended between two U-shaped, platinum wires that are position clamped at high loop gain by opto-electronic servos (*Biophys. J.* 64:A345, 1993). Resolution is 10 nN r.m.s. at 1.4 kHz bandwidth. The Fig. shows the tension response (upper traces) of an 81 µm long bundle of 3 myofibrils to step releases followed by ramps (lower traces). For each trace, the preparation is initially contracting at ~30 µM Ca^{2+}, ionic strength 200 mM, 20°C. On release force decreases, partially recovers during the following 20 ms, and then declines slightly during the imposed ramp length change. The quick decrease and recovery are attenuated with smaller step length changes suggesting that these phases are due to series compliance. After the initial recovery, the force during the ramp is lower for higher speeds of shortening. The force-velocity curve is concave upward as expected. Force recovers to ~80% of its pre-release value 500 ms after the ramp, indicating active tension redevelopment after shortening. The small deflection shown in the base-line (middle trace) is an artifact due to cross-talk between the wire servo systems. Distribution of shortening among the sarcomeres can be monitored dynamically from video signals. These results demonstrate that step-ramp length changes cause tension changes in myofibrils similar to those of muscle fibers. Supported by the MDA and HL15835 to the PMI.

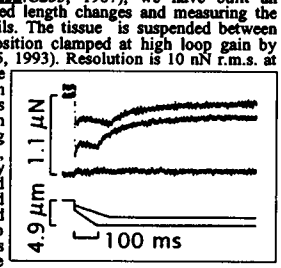

M-AM-A9

RIGOR TENSION DEVELOPED BY SINGLE SKINNED CARDIOMYOCYTE STRONGLY DEPENDS ON ADP AND PHOSPHOCREATINE.

((V. Veksler, P. Lechêne, R. Ventura-Clapier)) CJF 92-11 INSERM, Université Paris-Sud, Châtenay-Malabry 92296, France.

Ischemic rigor contracture develops in cardiac muscle at relatively high content of ATP. Dependence of rigor tension on MgATP concentration was studied using isolated skinned rat cardiomyocytes rather than fibers to avoid restrictions due to concentration gradients within the preparations. Triton X-100-treated cardiomyocytes were glued to glass electrodes, one of which was connected to a galvanometer. A feedback system allowed to measure force by recording the coil current necessary for preventing electrode movements. Maximal calcium-activated tension was 0.6-0.8 mg. At very low [Ca^{2+}] (pCa 7), as MgATP level decreased, in the absence of phosphocreatine (PCr), rigor tension started to rise at MgATP concentrations about 10 times higher than in the presence of 12 mM PCr. The pMgATP/tension curves of single cells usually had a complicated form which could not be fitted with a simple Hill equation. In the absence of PCr, 250 μM MgADP strongly potentiated rigor tension development in the range of [MgATP] 1 mM - 3 μM: at 100 μM MgATP, the tension was 3.3 times higher. These results indicate a myofibrillar compartmentation of adenine nucleotides influenced by bound creatine kinase. Therefore, in the absence of PCr, accumulation of ADP in the myofibrillar compartment could explain the rigor tension development at [MgATP] values which are much higher than Km for MgATP in myosin ATPase reaction.

M-AM-A10

MULTIPLE MUSCLE CROSSBRIDGE CYCLES PER ATP CYCLE

((C.Y. Seow & L.E. Ford)) Dept. of Med., U. of Chicago, Chicago, IL 60637

To determine whether the crossbridges of muscle produce more than one cycle of attachment, power-stroke, detachment per ATP hydrolyzed, we sought conditions that have little effect on the tension transients with more substantial effects on steady-state shortening. The addition of 5 mM ADP and 2 mM phosphate together produced such changes in skinned, rabbit psoas fibers at 1-2°C and pH 7.0. By itself, 5 mM ADP increased isometric force by 22% and decreased maximum velocity by 35% while 2 mM phosphate decreased isometric force by 15% without changing velocity. Together, both metabolites reduced maximum velocity by 36% while lowering isometric force and stiffness by only 2% and 4%, respectively. Analysis of the force-velocity curves suggested that the decreased velocity could be accounted for quantitatively by an internal load equivalent to 7% of isometric force, suggesting the detention of crossbridges in attached states (a/Po increased from 0.14 to 0.22 with no change in b [J. Gen. Physiol. **101**: 487, 1993]). By contrast, there was no evidence of such detention in the tension transients obtained with steps less than 9 nm/half-sarcomere. The early, rapid, (Phase 2) force recovery was slowed slightly, with no other changes in the transient tension responses. A 9.3-nm/half-sarcomere step also produced a 2% decrease in the late (Phase 4) force recovery. These findings suggest that the ADP and phosphate had little effect on the movements of bridges attached in the isometric state but that they slowed bridges after they have undergone one cycle of power stroke and detachment.

PROTEIN-LIPID INTERACTIONS

M-AM-B1

LYSOLIPID INHIBITION OF LOW PH-TRIGGERED VIRAL FUSION.

((L.V. Chernomordik, E.A. Leikina & J. Zimmerberg)) LTPB, NICHD, NIH, Bethesda, MD 20892. (Spon. by A. Krasnovsky)

We have previously reported that a single class of tightly regulated membrane components, lysolipids, reversibly inhibits membrane fusion for disparate biological fusion processes (L.V. Chernomordik et al., 1993, FEBS Lett. 318, 71-76). In order to elucidate fusion mechanisms and lysolipid effects in depth, we studied the fusion of biological membranes mediated by the specialized envelope proteins of baculovirus (gp64) and influenza virus (hemagglutinin). Lysolipids either added exogenously or produced *in situ* by phospholipase A2 treatment of cell membranes, inhibited pH-triggered syncytia formation. Lysolipids also decreased the baculovirus infection rate and lowered the buffer pH required for triggered syncytia formation. Inhibition of membrane fusion by a number of different amphipathic compounds cannot be explained by mere binding or incorporation into membranes. There is a limited time interval after a short low pH treatment during which the addition of lysolipid inhibited fusion. Thus lysolipids can act on pH-independent processes which follow the triggering of fusion. As in the case of baculovirus infected cells (S.S.Vogel et al., 1993, J. Biol. Chem. in press), lysolipids reversibly arrested influenza hemagglutinin mediated cell - cell fusion at a stage between triggering and membrane merger. Possible mechanism of a common mechanistic step in the fusion process arrested by the lysolipids will be discussed.

M-AM-B2

PROBING THE COMPLEX DIAMETER VS. TIME EXPANSION SIGNATURE IN MEMBRANE FUSION ZONES WITH OSMOTICALLY DEVELOPED MICROFORCES: PRELIMINARY STUDIES.

((Arthur E. Sowers, Jason D. Rosenberg, and R.A. Sjodin)) Departments of Biophysics and Pathology, UMAB, Baltimore 21201.

After a membrane fusion zone comes into existence between two cells, the two cell product may remain as two cells tethered to each other, or undergo a rounding up process that ends in a single large cell. We have recently discovered (Wu, Sjodin, and Sowers; BJ, accepted) that the rounding up process, which can be conveniently followed by measuring the fusion zone diameter vs. time relationship, displays a complex kinetic signature. Numerous lines of evidence show that the spectrin network is responsible for restraining this natural increase and suggest that i) the amount of the spectrin-dependent restraining force might be quantitatively estimated, and ii) this restraining force may play a complex regulatory role in cells. To probe this force and explore its regulation characteristics we induced membrane fusion between erythrocyte ghosts which were either re-loaded with 10 kDa dextran labeled with FITC or partially hemolyzed erythrocytes. The osmotic pressure difference expected to be developed across the plasma membrane from extra solute in the cytoplasmic compartment increased both the rate and extent of fusion zone expansion, thus suggesting that this may be a promising new approach to studying spectrin network mechanofunction. Supported by ONR grant N00014-92-J-1053 (AES) and NSF grant DCB-8916284 (RAS).

M-AM-B3

IN SITU ATTENUATED TOTAL REFLECTION FTIR STUDY OF pH-DEPENDENT STRUCTURAL AND FUNCTIONAL CHANGES OF RECONSTITUTED INFLUENZA HEMAGGLUTININ IN SUPPORTED BILAYERS

((S.A.Tatulian, P.Hinterdorfer, G.Baber and L.K.Tamm)) Dept. of Molecular Physiology and Biological Physics, University of Virginia School of Medicine, Charlottesville, VA 22908

Supported phospholipid bilayers with reconstituted influenza virus hemagglutinin (HA) were prepared on germanium internal reflection plates using the procedure described by P.Hinterdorfer, G.Baber and L.K.Tamm (see abstract in this issue). Polarized attenuated total reflection (ATR) Fourier transform infrared (FTIR) spectroscopy was used to characterize the pH-dependent structural changes of the HA and its capacity to bind phospholipid vesicles. The amide I' band was analyzed by curve fitting and yielded 23-26 % of α-helical conformation at pH 7.4, which is in good agreement with crystallographic data (I.A.Wilson, J.J.Skehel and D.C.Wiley 1981, *Nature* 289:366-373). The relative propensity of α-helix did not change significantly when the pH was lowered to 5. However, the ATR dichroic ratios (R^{ATR}) of the whole amide I' band, as well as that of the α-helical component, were shown to decrease significantly upon changing the pH from 7.4 to 5. The polarization results are consistent with an acid-induced change in orientation of the helical stem of HA from a vertical to a tilted orientation with respect to the plane of the membrane. Phospholipid vesicles composed of pure POPC, POPC/POPG (3:2), and POPC/cardiolipin (4:1) were bound to HA-bilayers. At pH 7.4, the amounts of bound lipid increased in the order: POPC < POPC/POPG < POPC/cardiolipin, indicating that both the target lipid charge and shape play a role in the vesicle-HA interactions. The binding of POPC/cardiolipin vesicles at pH 5 was approximately 2-fold more efficient than at pH 7.4, which may be accounted for by the exposure of the hydrophobic fusion peptide at low pH. The binding of all vesicles was accompanied with a decrease in R^{ATR} of the amide I' band to an extent proportional to the amount of bound lipid. The effects of acidic pH and vesicle binding on the conformation of HA, as judged from R^{ATR}, were additive. The lipid order parameter decreased upon injection of vesicles at pH 7.4 and was partly restored at pH 5. These results may be interpreted in terms of a low pH-induced partial fusion of target membranes with supported HA-bilayers.

M-AM-B4

RECONSTITUTED INFLUENZA HEMAGGLUTININ IN SUPPORTED PLANAR LIPID BILAYERS SELECTIVELY BINDS TARGET LIPID VESICLES AND INDUCES MEMBRANE FUSION AT LOW PH

((P. Hinterdorfer, G. Baber and L.K. Tamm)) Dept. of Molecular Physiology and Biological Physics, University of Virginia School of Medicine, Charlottesville, VA 22908

Influenza hemagglutinin (HA, strain A/PR/8/34) was purified and reconstituted into supported planar membranes in a two-step process: (1) virosomes were made by $C_{12}E_8$ detergent solubilization followed by detergent removal with Biobeads; (2) the virosomes were then transformed into "viroplanes", i.e. supported planar membranes which contained the viral membrane proteins. This step was accomplished by a spontaneous fusion of the virosomes with a phospholipid monolayer that was supported on a quartz microscope slide. The reconstitution of the HA into the planar membranes was followed by total internal reflection fluorescence microscopy (TIRFM) using fluorescein-labeled HA. By changing the solution concentration of HA, surface concentrations between 2.4 x 10^4 and 4.3 x 10^4 HA monomers per μm^2 were reached. Greater than 90% of all HA molecules were oriented with their large extra-viral domains facing away from the substrate toward the large aqueous compartment of the measuring cell. Binding experiments with conformation-sensitive monoclonal antibodies against HA established that the reconstituted HA could undergo the low-pH induced conformational change in the supported bilayer. Binding of vesicles containing the fluorescent lipid analog NBD-eggPE was also measured by TIRFM. Vesicle binding was promoted when sialic-acid containing gangliosides or negatively charged lipids were included in these target membranes. Membrane fusion of the HA bound vesicles was monitored by measuring long-range (over several μm) lateral diffusion coefficients of the lipids in the bound layer by fluorescence recovery after photobleaching (FRAP). The vesicles did not fuse at pH 7.4, but efficient vesicle fusion occured on the viroplanes after acidification of the environment with pH 5 buffer. This fusion reaction was only observed when the bound vesicles exceeded a critical threshold surface concentration.

M-AM-B5

RESONANCE X-RAY DIFFRACTION STUDIES ON ASYMMETRICALLY RECONSTITUTED CYTOCHROME B_5:DMPC MULTILAYERS ((D.W. Chester, Skita, V., Fischetti[§], R., Trumbore, M., Young, H.S.)) BSAC, Univ. of Connecticut Health Center, Farmington, CT. and Biostructures Institute[§], Philadelphia, PA.

Cytochrome b_5 serves as a redox pair for both fatty acid desaturases and cytochrome P_{450}. Electron transfer between these redox pairs is a rapid kinetic event suggesting some structural coordination of redox centers to facilitate efficient transfer. We have recently reported the asymmetrically reconstituted cytochrome b_5:DMPC profile structure [$\rho(z)$] at approximately 6 Å resolution. One conclusion drawn from the $\rho(z)$ is that the heme peptide is most likely oriented with the heme plane parallel to the bilayer surface. Anomalous x-ray scatter methods have been used to determine cytochrome c iron location in reconstituted photosynthetic reaction center preparations [Blasie et al., 1982]. Deisenhofer et al. [1984] later verified this location in the reaction center crystal structure, hence, demonstrating the structural power of anomalous scattering methods. In this work, we are attempting to evaluate the cytochrome b_5 redox center location and orientation in asymmetrically reconstituted DMPC membranes. Anomalous x-ray scattering studies were performed about the reconstituted cytochrome b_5 heme Fe^{+2} absorption edge [E_o=7.112 keV] with an energy range for data collection between E_o-200eV ≤ E_o ≤ E_o+200eV. Autocorrelation of both $\Delta I(s)$ and $|\Delta F(s)|^2$ for energies about E_o revealed a 114.4 Å vector centered across the 170.06 Å double membrane unit cell repeat. This vector places the heme iron atom 8-10 Å outside the outer phospholipid headgroup peak. Swelling the double membrane unit cell by approximately 2 Å resulted in a 1.3 Å shift of the vector to 115.7 Å demonstrating that the iron atom is moving with changes in the bilayer dimensions. Given the asymmetry of the heme placement within the cytochrome b_5 heme binding pocket, these data demonstrate that the heme plane lies approximately parallel to the bilayer surface. These studies were carried out on Beamline X9A at the NSLS, Brookhaven National Laboratories and supported by NIH-GM-15924.

M-AM-B6

HUMAN DEFENSINS FORM LARGE PORES IN ANIONIC LIPID BILAYERS. ((William C. Wimley, Michael E. Selsted and Stephen H. White)). Departments of Physiology and Pathology, University of California, Irvine, 92717.

Defensins are a family of small, globular, disulfide-stabilized antimicrobial peptides found in the dense granules of mammalian neutrophils which act by permeablizing the cell membranes of phagocytosed microorganisms. We have studied the interactions between one of the four human neutrophil defensins, HNP-2, and large unilamellar lipid vesicles. HNP-2, with a net charge of +6 per dimer, binds electrostatically to vesicles containing anionic phosphatidylglycerol (PG), but not to neutral vesicles. HNP-2 induces aggregation, and some fusion of PG vesicles, but without mixing of aqueous contents. Reduced HNP-2 does not induce PG vesicle fusion. Native HNP-2 causes PG vesicles (300 μM) to release entrapped markers, and the fractional leakage is a sigmoidal function of peptide concentration, with 50% leakage occurring at ~2.5 μg/ml (0.7 μM) HNP-2. Vesicle leakage induced by native HNP-2 occurs in an all-or-none manner, whereas reduced (non-native) HNP-2 induces partial, or graded, leakage of vesicle contents. Under conditions that released 100% of a small (440 Da) marker, only 85% of a fluorescent dextran of 4000 Da is released, and only 25% of a 20,000 Da dextran is released. These results suggest that HNP-2 forms multimeric pores in POPG vesicles that are no larger than approximately 20 Å. A model of the putative pore structure is presented based on these results and on the crystal structure of a human defensin. Supported by NSF and NIH GM46823. W.W. is supported by NIH GM14178.

M-AM-B7

2.5 Å STRUCTURE AND DETERGENT PROPERTIES OF PEPTIDES DESIGNED TO SOLVATE INTEGRAL MEMBRANE PROTEINS
((Christian E. Schafmeister, Larry J. Miercke, Robert M. Stroud))
University of California in San Francisco, CA 94143–0448

Several peptides have been designed, synthesized and characterized for use as detergents for solubilizing integral membrane proteins with the goal of obtaining large, well ordered, three dimensional crystals for atomic structure determination. The design of these peptides, termed peptitergents, was for amphipathic alpha–helices long enough to span the hydrophobic surface of a membrane protein and capable of maintaining solubility of the membrane protein by making hydrophobic contacts with the protein surface while exposing hydrophilic residues on the peptide to solvent. The first such peptitergent was found to crystallize by itself to form a four helix bundle and was capable of maintaining 85% solubility of bacteriorhodopsin and 60% rhodopsin solubility over a period of 2 days, however it was not capable of maintaining PhoE porin solubility (Science, in press). To improve membrane protein solvation, other peptides have been synthesized and their interaction with membrane proteins have been characterized by analytical centrifugation. The peptide structural data, and analysis of peptitergent properties will be presented and discussed.

M-AM-B8

LOW ANGLE X-RAY DIFFRACTION STUDIES OF NICOTINIC ACETYLCHOLINE RECEPTOR MEMBRANES FROM *TORPEDO CALIFORNICA*. ((Howard S. Young, Victor Skita, Mark Trumbore, Leo G. Herbette)) Biomolecular Structure Analysis Center, University of Connecticut Health Center, Farmington, CT 06030-2017

A profile structure has been determined for the nicotinic acetylcholine receptor (AChR) membrane from *Torpedo californica* to 15Å resolution using the technique of low angle x-ray diffraction. In the absence of a crystal structure for the AChR, an x-ray diffraction-based structural analysis of the native AChR-containing membranes has been underway in our laboratory. AChR-enriched membranes from *T. californica* have been purified to near homogeneity (≥65% AChR by weight protein) and fully oriented stacks of AChR membrane vesicles for x-ray diffraction have been prepared. These samples gave reproducible x-ray diffraction patterns indicative of a lattice organization perpendicular to the membrane plane, and a hexagonal lattice organization in the plane of the membrane. Analysis of the meridional diffraction pattern revealed a 450Å lattice spacing between stacked vesicle membrane pairs with a resolution of 9Å. In the plane of the membrane, the AChR molecules are organized in a hexagonal lattice with a center-to-center spacing of 80Å. At higher angle, the in-plane structure gave rise to diffraction characteristic of α-helix and acyl-chain packing. A profile structure has been determined for the AChR membrane from the experimentally observed intensity functions. Interpretation of the electron density profile gives the following: the cytoplasmic extension is 35Å, followed by a bilayer thickness of 43Å (headgroup to headgroup spacing) and a synaptic extension of 91Å for a molecular length of 169Å. While there are differences, this interpretation is consistent with radial density distributions of the AChR membranes as determined by cryoelectron microscopy of tubular crystals (Toyoshima and Unwin, 1990; Unwin, 1993). Experiments are in progress to verify these assignments using α-bungarotoxin and halogenated-agonists as probes for the locations of the acetylcholine binding sites. [Supported by Marion Merrell Dow, Cincinnati, OH, Univ. of Conn. Health Ctr. Grant, Farmington, CT, NIH 2P01H118608 and NIH RR01633]

ELECTRON TRANSFER

M-AM-C1

NEW TOOLS FOR UNDERSTANDING ELECTRONIC COUPLING IN PROTEINS
((J.J. Regan, S.S. Skourtis, J.N. Onuchic))
Department of Physics, University of California at San Diego,La Jolla, CA 92093.

A novel Green's function approach used to study the influence of conformation on donor–acceptor (D–A) matrix elements for several electron transfer proteins. The approach is nonperturbative and independent of the complexity of the electronic tight binding Hamiltonian used. The relation between the protein's structure and its function as an electron tunnelling medium is described by electronic contact and propagation maps.

In light of this model, results for cytochrome c and azurin are presented. For each protein we analyze the coupling statistics that arise from the folded structure, we compute electronic contact and propagation maps, and we calculate propagation and interference effects between different protein structural elements. These results are used to characterize the electron transfer ability of each protein as a function of tunnelling energy and the D–A pair.

Also, these results are compared to pathway analysis. Pathways and pathway families are similarly defined on a green's function foundation. The two techniques have important differences, and thus provide a complementary set of tools for protein analysis.

Work supported by the NSF (grant MCB-9018768) and by the NIH (training grant 5T32 GM08326–03).

M-AM-C2

PROTEIN ELECTRON TRANSFER: A NOVEL APPROACH FOR THE DESCRIPTION OF DONOR-ACCEPTOR COUPLING
((S. S. Skourtis, J.J. Regan, J.N. Onuchic))
Department of Physics, University of California at San Diego, La Jolla, CA 92093.

We propose a novel Green's function approach for analyzing the effects of conformation on electron transfer matrix elements in proteins. This approach allows the analysis (at all levels of detail) of the contributions of different protein structural elements to the electronic coupling between donor and acceptor. It is nonperturbative and it is also suitable for describing electronic propagation and interference effects analytically or semianalytically.

We define electronic contact maps and electronic propagation maps which can be used to interpret the effect of the protein's conformation on the total donor-acceptor coupling. These maps relate the protein's structure to its function as an electron tunnelling medium. The electronic contact maps reflect the effect of the protein's folded conformation on the electronic coupling hamiltonian. The electronic propagation maps describe the influence of conformation on the donor-acceptor coupling in terms of electronic propagation and scattering events. The above methods are used to the study and compare donor-acceptor matrix elements for several electron transfer proteins.

Work supported by the NSF (grant MCB-9018768) and by the NIH (training grant 5T32 GM08326–03).

M-AM-C3

LONG RANGE ELECTRON TRANSFER REACTIONS IN A METHYLAMINE DEHYDROGENASE-AMICYANIN-CYTOCHROME c-551i COMPLEX. ((V.L. Davidson, H.B. Brooks, L. Chen, R. Durley and F.S. Mathews)) Univ. of Miss. Med. Ctr., Jackson MS 39216 and Washington Univ. School of Med., St. Louis MO 63110.

A quinoprotein methylamine dehydrogenase [MADH], a type I copper protein, amicyanin, and a cytochrome, c-551i, form a physiologic complex in which electrons are transferred from tryptophan tryptophylquinone [TTQ] to copper to heme. Crystals of a complex of these proteins have been analyzed by x-ray diffraction. In this crystallized complex the distance from the edge of TTQ to copper is 9.4 Å and that from copper to the iron of the heme group is 24.8 Å. The electron transfer [ET] reaction from reduced TTQ to amicyanin was studied by stopped-flow spectroscopy. At temperatures ranging from 10-50°C, the ET rate varied from 2-55 s^{-1}. Fits of these data to the Marcus equation indicated that a reorganizational energy of 2.3 eV and electronic coupling of 11.7 cm^{-1} were associated with this ET reaction. Steady-state kinetic studies of the reduction of cytochrome within the complex yielded a kcat at 30°C of 9 s^{-1}, which may be considered the minimum value for the rate of ET from copper to heme. From these structural and kinetic data it has been possible to predict pathways of ET within the complex, evaluate their likelihood and speculate about conformational changes within the protein complex that may have to occur to facilitate the ET reactions. Supported by NIH grant GM-41574.

M-AM-C4

BINDING AND ELECTRON TRANSFER REACTIONS BETWEEN METHANOL DEHYDROGENASE AND CYTOCHROME *c*-551i. ((T.K. Harris* and V.L. Davidson)) University of Mississippi Medical Center, Jackson, MS 39216-4505

The quinoprotein methanol dehydrogenase and cytochrome *c*-551, form a physiologic complex in which electrons are transferred from pyrroloquinoline quinone to heme. The reoxidation of methanol dehydrogenase by the cytochrome was studied by stopped-flow spectroscopy. The rate constant for the electron transfer reaction and the dissociation constant for complex formation were each determined at temperatures ranging from 20° to 50° C. The electron transfer rates varied from 1.4 to 4.6 s^{-1}. Analysis of the electron transfer reaction by Marcus theory yielded values of 1.86 eV for the reorganizational energy and 0.071 cm^{-1} for the electronic coupling, and predicted a theoretical distance between redox centers of 15 Å. Kinetically determined dissociation constants correlated well with a K_d of 375 μM which was determined in a direct ultrafiltration binding assay. Thermodynamic analysis of the dissociation constants indicated the importance of the hydrophobic effect in complex formation. The ionic strength dependence of the kinetically determined dissociation constants also suggested that electrostatic interactions play a role in complex formation as well. Interestingly, k_{ET} was ionic strength dependent. This implies that k_{ET} may contain a contribution from some rearrangement of the proteins after a nonoptimal collision to produce the most efficient orientation for electron transfer. This would be consistent with the notion that the large reorganizational energy reported for the temperature dependent studies on k_{ET} is due to such a rearrangement. Supported by NIH grant GM-41574.

M-AM-C5

THE REACTION OF CYTOCHROME $\underline{caa_3}$ OXIDASE FROM *BACILLUS SUBTILIS* WITH OXYGEN ((Bruce C. Hill)) Dept. Biochem., Queen's University, Kingston, ON K7L 3N6 Canada

B. subtilis has two different heme A-containing terminal oxidases. The cytochrome $\underline{caa_3}$ oxidase has a cytochrome $\underline{c}$ domain within the sequence of subunit II. The fully reduced enzyme reacts with CO to form a ferrocytochrome a_3-CO species that is photosensitive, and has a 'dark' off rate of 0.1 s^{-1}. Thus, the enzyme is suitable for study by stopped-flow, flash-photolysis to investigate its reaction with O_2. At 604 nm, the α-band of cytochrome $\underline{a}$, four phases are observed in the reaction with O_2. The first three phases taking up 25% of the absorbance change are complete in 3 ms, and the remainder is complete in 20 s. At 400 μM O_2 absorbance intially decreases at a rate of 2.2×10^4 s^{-1}, then absorbance increases at 5.8×10^3 s^{-1} and in the third phase absorbance decreases at 650 s^{-1}. At 550 nm, the α-band of cytochrome $\underline{c}$, four phases are also resolved with 67% of the absorbance change complete in 3 ms and the remainder in 1 s. The same rates observed at 605 nm occur in the first 3 ms at 550 nm, but with different absorbance contributions to each kinetic phase. These results show that cytochrome $\underline{c}$ in the $\underline{caa_3}$ complex participates in the single turnover reaction of the oxidase with oxygen. (Supported by the Natural Sciences and Engineering Research Council of Canada).

M-AM-C6

UNDECAGOLD LABELING OF CYTOCHROME OXIDASE: THE SITE OF SUBUNIT III IDENTIFIED IN TWO-DIMENSIONAL CRYSTALS ((J. Crum, K.J. Gruys, P.A. Frey and T.G. Frey)) Dept. of Biology San Diego State University, San Diego, CA 92182. Institute for Enzyme Research, University of Wisconsin, Madison, WI 53706.

Mitochondrial cytochrome *c* oxidase is a complex integral membrane protein which catalyzes the terminal step in electron transfer to O_2. Of the 13 known polypeptide components in the enzyme isolated from beef heart mitochondria, only the two largest, I and II, have known functions, binding two heme *a* and two Cu ions. Subunit III has been proposed to play a role in either regulation of proton pumping or in assembly of the protein complex. Subunit III contains a single reactive cysteine sulfhydral, Cys-115, which can be selectively labeled with hydrophilic sulfhydral reagents. We have previously shown that a monomaleimide derivative of a water soluble undecagold cluster compound reacts selectively with subunit III in two-dimensional crystals of cytochrome oxidase dimers. We have now identified the site of undecagold cluster binding (and hence the site of subunit III) in projection images of cytochrome oxiase dimers obtained by electron microscopy of two-dimensional crystals. The molecular outline of a dimer in projection along a membrane normal can be approximated as a rectangle 44 Å by 82 Å. The two undecagold binding sites in each dimer are found to be 60-70 Å apart near opposite corners of the rectangular molecule. This an area of close contact between the two monomers based upon our recent model for the arrangement of cytochrome oxidase monomers within a dimer. It is also consistent with the known proximity of Cys-115 of subunit III to the cytochrome *c* binding site which we have recently located by cryoelectron microscopy of two-dimensional crystals.

M-AM-C7

A NON-REDOX ACTIVE METAL BINDS NEAR THE ACTIVE SITE OF CYTOCHROME *c* OXIDASE. ((J.P. Hosler, M. Espe, Y. Zhen, G.T. Babcock and S. Ferguson-Miller)) Departments of Biochemistry and Chemistry, Michigan State University, East Lansing, MI 48824

Non-redox active, EPR-silent metals (Mg and Zn) are bound by mitochondrial cytochrome *c* oxidases, but their locations and functions are not clear. Variable amounts of Mn are tightly bound to the aa_3-type cytochrome *c* oxidase of *Rhodobacter sphaeroides*, and easily observed in the $g = 2.0$ region of the EPR spectrum. The bound Mn is not exchangeable in the fully assembled protein. The amount of bound Mn directly correlates with the [Mn] to [Mg] ratio in the culture medium, such that oxidase containing no EPR detectable Mn or oxidase containing near stoichiometric levels of Mn (0.7 mol/mol aa_3) can be prepared. When the amount of bound Mn is varied, electron transfer activity is not altered, suggesting that Mg may occupy this site in the absence of Mn and maintain protein structure. We propose that Mn has affinity for a site in the bacterial enzyme that is homologous to the Mg binding site of mitochondrial cytochrome *c* oxidase. Mutants of conserved residues H411 and D412, located in an extramembrane loop connecting transmembrane helices IX and X of subunit I, fail to bind Mn, and show loss of activity. ESEEM analysis of the wild-type enzyme shows the presence of one nitrogenous ligand to the Mn, presumably H411. Since H411 and D412 are closely associated with the heme a_3-Cu_B center (Hosler *et al.* (1993) *Biochem.*, in press), these results suggest a central structural role for Mn/Mg site.

M-AM-C8

UNCOUPLER INHIBITION OF OXYGEN INTERMEDIATE FORMATION IN CYTOCHROME OXIDASE. ((H. James Harmon)) Oklahoma State University, Stillwater, OK 74078

The reaction of oxygen with ferrous cytochrome oxidase in intact beef heart mitochondria capable of maintaining pH differences across the membrane begins with the binding of molecular oxygen to cyt a_3 (cmpd A formation) following flash photolysis of carboxyoxidase. Following formation of cmpd A, oxidation of the oxidase and reduction of O_2 yields 2 species of the "peroxy" intermediate (cmpds B). The first (cmpd B_{450}) is detected by absorbance decrease at 450 nm; the decrease in 441 nm absorbance heralds formation of B_{441}. In the presence of CCCP at pH 7, cmpd B_{450} but not B_{441} is observed. In the absence/presence of CCCP matrix pH is approx 5 and 7 resp.; this suggests that B_{441} is a protonated intermediate and that the B_{450}-B_{441} conversion involves a matrix proton. That B_{441} forms at pH 5 but not at pH 9 in the presence of CCCP is further evidence of formation of a protonated intermediate and that the pK of the conversion is below pH 7. Assignment of 441 and 450 nm absorbances as cyt $\underline{a}$ and $\underline{a_3}$, resp., suggests that protonation occurs after 2 electrons are transferred to O_2 and prior to cyt $\underline{a}$ oxidation, in agreement with other reports.
Supported by a grant from the Oklahoma Center for the Advancement of Science and Technology.

M-AM-C9

STUDIES ON THE SUBUNIT 10 OF CYTOCHROME BC_1 FROM *Saccharomyces cerevisiae*. (S. Uribe, U. Brandt and B. L. Trumpower) Dept of Biochemistry, Dartmouth Medical School, Hanover, NH 03755.

Recently, a tenth subunit of the cytochrome bc_1 complex from *S. cerevisiae* was described. This subunit has a molecular weight of 8.5 kDa and its genomic sequence has been determined. The gene for subunit 10 was deleted from the yeast genomeusing a selectable marker and the properties of the mutant were studied. The haploid deletion strain did not show a growth phenotype. In addition, the cytochrome spectra were indistinguishable in the wild type and the mutant. However, when the quinol-cytochrome c redox activity of mitochondria from either strain was tested, a decrement of about 40% in the enzymatic activity of cytochrome bc_1 was detected in the deletion. When cytochrome bc_1 was purified from mitochondria, a decrease in the content of the Rieske iron-sulphur protein was observed. The loss of ISP occurred during isolation because the concentration of ISP in mitochondria, as determined by Western analysis using monoclonal antibodies. Our results suggest that the protein described is subunit 10 of the mitochondrial bc_1 complex and that it participates in the stabilisation of the interaction of ISP with the rest of the complex

M-AM-C10

BINDING OF DCCD AND NCD-4 TO ASPARTATE-160 ON HELIX cd OF CYTOCHROME B FROM YEAST MITOCHONDRIA. Y. Wang and D.S. Beattie, Dept. Biochem. West Virginia Univ., Morgantown, WV 26506.
The cytochrome bc_1 complex of the mitochondrial electron transport chain catalyzes electron transfer from ubiquinol to cytochrome c coupled to electrogenic proton translocation. Dicyclohexylcarbodiimide (DCCD), the well-established carboxyl-modifying reagent, and its fluorescent analogue, N-cyclohexyl-N'-[4-(dimethylamino)naphthyl]carbodiimide (NCD-4), inhibited proton translocation 70% in the bc_1 complex incorporated into proteoliposomes with a 25% inhibition of electron transfer and were bound to cytochrome b. Proteolytic cleavage of [14C]DCCD labeled cytochrome b with either trypsin or SV8 protease produced radiolabeled peptides which were sequenced. The results indicated that [14C]DCCD bound to aspartate-160 present in the amphipathic helix cd of cytochrome b. Peptides of the same molecular weight were fluorescent when NCD-4 labeled cytochrome b was subject to digestion suggesting that DCCD and NCD-4 are bound to the same aspartate residue. The fluorescence of NCD-4 bound to the bc_1 complex reconstituted into proteoliposomes was quenched almost equally by CAT-16, an amphiphilic spin label that intercalates at the membrane surface, and by the nitroxide derivative of stearic acid, 5-doxylstearic acid. Significant quenching of the NCD-4 fluorescence was also observed with 7-doxylstearic and 12-doxylstearic acids. At higher concentrations, the hydrophilic membrane-impermeant quenchers, CAT-1 and D-569 also quenched the fluorescence of the NCD-4. These results suggest that aspartate-160, the binding site for NCD-4 on amphipathic helix cd of cytochrome b, is localized within the membrane where it is shielded from the external aqueous environment.

ACETYLCHOLINE RECEPTORS

M-AM-D1

COMPETITIVE ANTAGONISTS BRIDGE THE α–γ SUBUNIT INTERFACE OF THE ACETYLCHOLINE RECEPTOR THROUGH QUATERNARY AMMONIUM-AROMATIC INTERACTIONS. ((D.X. Fu and S.M. Sine)) Department of Physiology & Biophysics, Mayo Clinic, Rochester, MN 55905

Common to a broad class of competitive antagonists of the acetylcholine receptor (AChR) are two quaternary ammonium groups separated by 11 Å. We recently demonstrated that Y198 of the α-subunit and Y117 of the γ-subunit affect binding of the antagonist dimethyl-d-tubocurarine (DMT). To test the hypothesis that DMT interacts directly with these tyrosines and therefore bridges the α–γ subunit interface, we introduced a series of mutations at each position and expressed either one or both mutant subunits in $\alpha_2\beta\gamma_2$ AChRs in 293 HEK cells. Binding of DMT, measured by competition against the initial rate of ^{125}I-α-bungarotoxin binding, reveals that changes in binding energy for double subunit mutants approximately equals the sum of changes in binding energy for single subunit mutants. These results support direct contributions of both tyrosines to stabilization of two distinct parts of DMT. For both the α- and the γ-subunit mutants, the side chain specificity of DMT affinity is consistent with aromatic-quaternary interactions: for α-198 the rank order of affinities is F>C>T, and for γ-117 the order is F>T>R. To further establish stabilization through aromatic-quaternary interactions, we studied binding of two more bis-quaternary antagonists, pancuronium and gallamine. Both of these ligands are affected similarly to DMT for the entire panel of α- and γ-subunit mutations. Because these three ligands have essentially different backbones but have in common two quaternary ammonium groups, we conclude that αY198 and γY117 stabilize quaternary ammonium groups of these competitive antagonists, and therefore that they bridge the α–γ subunit interface.

M-AM-D2

SINGLE-CHANNEL KINETICS OF MOUSE AChR: MUTATIONS OF α-SUBUNIT RESIDUES Y198, Y190, Y93, and D200. ((Y. Zhang, J. Chen, G. Akk, S. Sine*, and A. Auerbach)) Dept. Biophysical Sciences, SUNY at Buffalo, NY 14214 and *Dept. Physiol Biophysics, Mayo Foundation, Rochester, MN 55905

We have recorded and modeled single-channel currents (Horn-Lange method; concerted activation scheme) from wt and mutant mouse AChR, expressed in oocytes or HEK 293 cells. The fitted activation rates adequately describe macroscopic equilibrium binding and dose-response profiles. The wt opening rate is ~20,000 s^{-1} and the closing rate is ~100 times slower. The affinity for ACh differs about 2-fold at the two binding sites (K_{d1}=41 μM and K_{d2}=77 μM). The rates of association and dissociation are, respectively, 4- and 7-fold faster at the lower affinity site. The mutant **Y198F** opening rate is 2-3 times slower than the wt, but has a closing rate that is similar to the wt. The association rates to both sites are ~10-fold lower in the mutant, but only dissociation from the high affinity site is reduced, again about 10-fold. Mutants **Y198S**, **Y198T**, and **Y190F** were not modeled, but have apparent open times that are ~4 times shorter than wt. Mutant **Y93F** exhibits ~20-fold reduced association rates at both binding sites, but, like Y198F, only significantly reduces dissociation (~10-fold) at the high affinity site. This mutant also has about a 4-fold slower opening rate than wt, but essentially the same closing rate. Preliminary results suggest that **D200N** has a drastically slower opening rate, by at least 40-fold, with little change in other activation rates. The results suggest 1) the binding sites are nonequivalently affected by mutations 198F and 93F, 2) the channel opening rates are influenced by several residues, and 3) closing rates are only modestly influenced by mutations near the binding site. Alternative interpretations of wt and mutant kinetic behaviors were obtained by modeling with a stepwise activation scheme. (thanks to Jim Patrick and Gary Yellen; supported by grants from NSF, NIH and MDA)

M-AM-D3

SINGLE CHANNEL KINETICS OF MOUSE ACHR δW57Y
((Yinong Zhang, Jian Chen and Anthony Auerbach)) Department of Biophysical Sciences, SUNY at Buffalo, NY 14214. (Spon. by M. Slaughter)

Recent studies have indicated that agonist binding sites of nAChR are formed by α/δ and α/γ subunit pairs, with the α/δ site having a higher affinity for agonists. In wt *Torpedo* nAChR δ tryptophan 57 was photolabelled by dTC suggesting that it may be near the binding site (Chiara and Cohen, Biophys. Abstr., 1992). We have replaced this tryptophan with tyrosine (δW57Y), expressed mutant mouse AChR in oocytes and HEK 293 cells, and have studied its kinetic behavior by single channel analysis. The dose-response profile of δW57Y, measured by Popen within clusters vs. ACh concentration, showed an EC_{50} of 19 μM (11 μM in wt) and a maximum of 0.96 (0.98 in wt), i.e. a less than 2-fold shift towards higher ACh concentration relative to wt. Idealized single channel currents were fitted to the standard, four state concerted model of activation by the Horn-Lange maximum likelihood algorithm. There were two significant changes in the mutant, compared to the wt. First, the opening rate was about 5 times slower (no change in the closing rate). Second, the dissociation from the higher affinity (α/δ) site was slowed more than 10-fold , while the association rate dropped only 2-fold (Kd=5 μM in mutant and 25 μM in wt). There was no difference in the binding properties of the lower affinity (α/γ) site. The rate differences between mutant and wt AChR are substantial, but, because they have opposite influences on Popen, combined they produce only small changes in the dose-response profile. This study indicates that 1) a mutation in δ can alter the channel opening rate, 2) the α/δ binding characteristics were altered in this mutant with no effect on binding to the α/γ site, 3) major kinetic effects may not be detected with macroscopic dose-response studies. (Supported by grants from NIH and MDA)

M-AM-D4

EFFECTS OF ETHANOL ON ACH RECEPTOR CHANNELS.
((J.P. Dilger, Y. Liu, J. F. Roper and R.J. Bradley)) Dept. of Anesthesiology, SUNY, Stony Brook, NY 11794, Dept. of Pharmacology, UAB, Birmingham, AL 35294 and Dept. of Psychiatry, LSU, Shreveport, LA 71130.

Ethanol decreases the *apparent* dissociation constant for acetylcholine (ACh) at the nicotinic ACh receptor (Brain Res. 295:101, '84; Biochim. Biophys. Acta 987:95; '89). This could be due to either an increase in the affinity of the receptor for ACh or to an increase in the efficacy of ACh as an agonist. To distinguish between these alternatives, we studied the effects of (10-3000 mM) ethanol on AChR channels in outside-out patches from BC3H-1 cells using single channel recording and rapid perfusion techniques. When 0.2 μM ACh or 1 μM decamethonium (Deca) is used to activate channels, 300 mM ethanol increases the frequency of channel opening 2-fold and increases the channel open and burst durations 2-fold. Ethanol (300 mM) shifts the ACh dose-response curve to the left by 10 μM. Ethanol does not increase the peak open probability induced by 100 μM ACh (≈0.90). However, ethanol increases the peak open probability induced by 100 μM Deca (a partial agonist; Synapse 13:57, '93) from 0.015 to 0.05. In addition, 300 mM ethanol decreases the onset time of the current response to 10 mM ACh by 40%. We conclude that the major effect of ethanol is to increase the efficacy of agonists by increasing the opening rate and decreasing the closing rate of the gate of the channel.
Supported by GM42095 (JPD) and AA09140 (RJB).

M-AM-D5

LOCALIZATION OF THE AGONIST SELF-INHIBITORY BINDING SITE ON THE NICOTINIC ACETYLCHOLINE RECEPTOR. ((H.R. Arias and D.A. Johnson) Inst. Invest. Bioquím., Bahía Blanca-8000, Argentina, and Div. Biomed. Sci. and Dept. Neurosci., Univ. Calif., Riverside, CA 92521-0121. (Spon. by R. Zidovetzki)

High concentrations of nicotinic agonists have been previously shown to inhibit ion fluxes through the nicotinic acetylcholine receptor (AChR). To determine whether or not this effect is mediated through agonist binding to one of two noncompetitive inhibitor sites on the AChR, we measured the ability of three nicotinic agonists, acetylcholine (ACh), carbamylcholine (CCh) and suberyldicholine (SubCh), to inhibit the binding of ethidium and quinacrine, fluorescent noncompetitive inhibitors. The inhibition constants (K_i) for ACh, CCh and SubCh to inhibit phencyclidine-sensitive ethidium binding were 8, 11 and 109 fold greater than for the inhibition of phencyclidine-sensitive quinacrine binding, respectively. Thus, the rank order of the sensitivity of quinacrine binding to agonist displacement is: SubCh >> ACh > CCh. This rank order is essentially identical to the published rank order of these agonists for self inhibition of ion fluxes. These results indicate that the low-affinity agonist binding site, at least, partially overlaps with the quinacrine binding site. Because quinacrine appears to bind within the transmembrane domain, agonist self inhibition of ion flux is via an allosteric, not stearic, mechanism.
(Supported by a CONICET fellowship and by NSF grant IBN-9215105)

M-AM-D6

SUPPRESSION OF INWARD RECTIFICATION IN α7 NEURONAL NICOTINIC ACh RECEPTORS
((Ian C. Forster)) Department of Physiology, University of Zurich, CH-8057, Switzerland

A consistent feature of neuronal nicotinic ACh receptors (nAChRs) is strong inward rectification. Using a two electrode voltage clamp and voltage step protocols, the inward rectification of α7 neuronal nAChRs expressed in *Xenopus* oocytes was investigated. The instantaneous IV curve of the wild type receptor showed rectification for positive membrane potentials, similar to the behaviour observed under steady state conditions for this receptor (Couturier et al.,(1990) Neuron, 5, 847-856). In contrast, rectification was absent in α7 mutants in which the glutamic acid residues, comprising the negatively charged intermediate ring at the cytoplasmic end of the putative channel region M2, were replaced by alanines. One candidate for rectification in nAChRs is block by internal Mg^{2+}. When either of the Mg^{2+} chelators Na_2ATP or CDTA were pressure injected into oocytes expressing the wild type receptor, rectification was reduced in a dose dependent manner. With an estimated internal free Mg^{2+} of less than 0.1 μM, some non-linearity still remained in the instantaneous IV curve for positive potentials. These findings confirm that Mg^{2+} blocking contributes significantly to rectification in these receptors and suggest that the intermediate ring in the wild type receptor pore acts as a Mg^{2+} blocking site.
Supported by Swiss National Science Foundation grant 31 36552-92

M-AM-D7

DIPOLAR FLUORESCENCE ENERGY TRANSFER BETWEEN THE LIPID MEMBRANE AND THE PHENCYCLIDINE-SENSITIVE ETHIDIUM BINDING SITE ON THE NICOTINIC ACETYLCHOLINE RECEPTOR. ((D. A. Johnson and J. M. Nuss)) Div. of Biomedical Sciences and Dept. of Chemistry, University of California, Riverside 92521-0121.

Although high-affinity noncompetitive inhibitors of the nicotinic *Torpedo* acetylcholine AChR (AChR) appear to bind at multiple sites in a mutually exculsive manner, most evidence suggests that these binding sites are localized within the transmembrane domain of the AChR. To confirm that ethidium (EB), a fluorescent noncompetitive inhibitor, binds within the AChR transmembrane domain, we measured the transverse distance between AChR-bound EB and the lipid membrane. Specifically, we measured the quenching of phencyclidine-sensitive EB fluorescence due to dipolar fluorescence energy transfer to membrane-partitioned N-(Texas Red® sulfonyl)-5(and 6)-dodecanoylamine (C_{12}-Texas Red). The fluorescence energy transfer was of a magnitude consistent with AChR-bound EB being ~45Å above the plane of the membrane-partitioned C_{12}-Texas Red. Given the cross-sectional diameter of the AChR transmembrane domain (~55Å) and our previous measurements (1) of the average distance between the EB binding site and the acetylcholine binding sites (21-40 Å) and (2) of the transverse distance between the AChR-bound dansyl-C_6-choline and the membrane surface (~35Å), the present results suggest that the EB binds at a site significantly above (~40Å) the transmembrane domain. (Supported by NSF grant IBN-9215105)

M-AM-D8

CHEMICAL KINETIC STUDIES OF NEUROTRANSMITTER RECEPTORS BY LASER-PULSE PHOTOLYSIS IN THE MICROSECOND-TO-MILLISECOND TIME REGION
((L. Niu and G.P. Hess)) Biochemistry, Molecular & Cell Biology, Cornell University, Ithaca, NY 14853

A super-family of membrane-bound proteins regulates the transmission of signals at the junctions between cells of the mammalian nervous system. Upon binding a specific neurotransmitter these receptor proteins form transient (~1 ms) channels through which inorganic ions flow, leading to a change in the transmembrane voltage of a cell. A newly developed laser-pulse photolysis technique, with a µs time resolution, allows one to determine the rate constants for both the formation and closing of the transmembrane channel, the dissociation constant for the ligand-binding site that controls channel opening, and the concentration of the receptor in the cell membrane, and gives information about the rate of transient inactivation (desensitization) of the receptor. The use of the chemical kinetic method will be illustrated by experiments with the nicotinic acetylcholine receptor in BC_3H1 muscle cells. The technique allows one to determine the binding constants of inhibitors to the closed- and open-channel forms independently. A number of compounds, including local anesthetics and abused drugs, are believed to inhibit the receptor by entering its open channel and physically blocking it. However, three of the inhibitors tested were found to bind to the closed-channel form of the receptor, presumably to a specific regulatory site. With one inhibitor we obtained evidence that the receptor:inhibitor complex can still form a transmembrane channel, but that a slow subsequent transition induced by the inhibitor leads to an inactive receptor form. (This work was supported by grants from the National Institutes of Health.)

HEME PROTEINS I

M-AM-E1

DETECTION OF RECOMBINATION INTERMEDIATES FOR PHOTODISSOCIATED CO MYOGLOBIN BY TIME-RESOLVED RESONANCE RAMAN SPECTROSCOPY.
((S.Nakashima*, T.Kitagawa*, J.S.Olson†))*Institute for Molecular Science,Okazaki 444 Japan.†Dept. of Biochemistry and Cell Biology, Rice University, Houston, Texas 77251

Time-resolved resonance Raman experiments of recombined species of photodissociated CO sperm whale myoglobin and its mutants have revealed a transient "open" form at ambient temperatures for the first time. The Fe-CO stretching band(ν_{Fe-CO}), which is sensitive to the heme environment, appeared at 509cm^{-1} in the equilibrium state. This band was absent just after photodissociation(Δt=0ns), but gave a broad band around 504cm^{-1} at Δt=1µs and was 65% restored with a frequency shift to 509cm^{-1} by Δt=1ms. These bands all showed isotopic frequency shifts characteristic of ν_{Fe-CO} stretching. H64Y, H64YV68F, H64W and H64WL29F mutants gave the ν_{Fe-CO} band at 493, 490, 496 and 520 cm^{-1} in the equilibrium states, respectively. Although their equilibrium frequencies differ, their transient bands all appeared in the same frequency region, around 500cm^{-1}. Thus in their transient states the heme pocket polarities of these distal mutants are very alike, suggesting that the distal residues have swung out of the heme pocket in the transient states.

M-AM-E2

VISCOSITY DEPENDENCE OF OXYGEN ESCAPE FROM RESPIRATORY PROTEINS AS A FUNCTION OF COSOLVENT MOLECULAR WEIGHT.
((D. Lavalette[a], C. Tetreau[a], B. Gavish [b] and S. Yedgar[b]))
a)INSERM U350,Institut Curie, 91405-Orsay France. b) Biochemistry Department, The Hebrew University, Jerusalem 91010, Israel.

Laser photodissociation of respiratory proteins is followed by fast geminate recombination competing with escape of the oxygen molecule into the solvent. The escape rate from Myoglobin or Hemerythrin exhibits a reciprocal power-law dependence on viscosity [Beece & al., 1980; Lavalette & Tétreau, 1988].We have re-investigated oxygen escape from Hemerythrin using a number of viscous cosolvents of varying molecular weight, from glycerol to dextrans up to 1MDa. In isoviscous solutions, the strong viscosity dependence observed with small cosolvents is progressively reduced upon increasing the cosolvent's molecular weight and disappears at molecular weights greater than about 100 kDa. Thus viscosity is not a suitable independent parameter to describe the data. The power-law dependence of the rate constant is a function of the cosolvent's molecular weight, suggesting that local protein-solvent interactions rather than bulk viscosity are affecting protein dynamics.

D. Beece & al., 1980, Biochemistry, 23, 5147-5156.
D. Lavalette & C. Tétreau, 1988, Eur. J. Biochem., 177, 97-108.

M-AM-E3

pH DEPENDENCE OF HEMOGLOBIN CONFORMATIONAL DYNAMICS PROBED BY UV RESONANCE RAMAN SPECTROSCOPY.
((V.Jayaraman, I.Mukerji, K.R.Rodgers, T.G.Spiro)) Dept. of Chemistry, Princeton University, Princeton, NJ 08544.

The Bohr effect in hemoglobin (Hb) arises from changes in the pK_a values of certain residues upon ligand binding. Among these are the α20, α89, β143, and β146 histidines. Phenomenologically this leads to a shift in the quaternary equilibrium towards the T structure on acidification. The effect of Bohr protons on the quaternary structure and on the dynamics of R-to -T state transition of Hb were investigated using UV resonance Raman spectroscopy. The 230 nm excited resonance Raman spectra of the Hb T and R states at pH 5.8 and pH 9 are similar to those at pH 7.4. This indicates that the structures, specifically the environments of tryptophan (Trp) and tyrosine (Tyr) residues, are not altered significantly upon protonation or deprotonation of the Bohr residues. The dynamics of the R-to-T transition were studied at pH 5.8 and pH 9 using 230 nm Raman excitation to probe the changes after photodissociation of HbCO. The time resolved spectra show sequential tertiary and quaternary conformational changes at all the three pH conditions. The transient spectra are indicative that the overall pathway of the R-to-T transition are qualitatively similar at the three pH values. However, the kinetics of the R-to-T transition is accelerated when the protein is at a lower pH.

M-AM-E4

RESONANCE RAMAN SPECTROSCOPY OF GUANYLYL CYCLASE REVEALS DISPLACEMENT OF DISTAL AND PROXIMAL HEME LIGANDS BY NO
((Songzhou Hu[a], Anita E. Yu[b], Judith N. Burstyn[b], and Thomas G. Spiro[a])) [a]Department of Chemistry, Princeton University, Princeton, NJ 08544; [b]Department of Chemistry, University of Wisconsin-Madison, Madison, WI 53706.

We present resonance Raman (RR) spectra of bovine soluble guanylyl cyclase (sGC) which establish that NO does displace a proximal ligand, probably histidine. The NO adduct shows RR frequencies for the porphyrin skeletal modes ν_3 (1508 cm^{-1}) and ν_{10} (1646 cm^{-1}), which are characteristic of 5- (5-c) rather than 6-coordinate (6-c) heme. When CO binds to Fe[II] heme in sGC, the Fe-CO stretching RR band is at 495 cm^{-1}, indicative of a non-polar binding pocket and a histidine proximal ligands. The resting enzyme, as well as the CO adduct, show laser power-dependent ν_3 bands at 5-c high-spin (1468 cm^{-1}), as well at 6-c low-spin (~1500 cm^{-1}) frequencies. Thus the resting enzyme has an endogenous distal ligand, which must be displaced upon adduct formation. Both ligand displacements, proximal and distal, may play a role in activation of the enzyme.

M-AM-E5

Effect of disordered hemes and dimerization in isolated α-subunits of hemoglobin detected by time resolved fluorescence spectroscopy.
Zygmunt Gryczynski, Clara Fronticelli, Enrico Gratton, Jacek Lubkowski and Enrico Bucci. Dept of Biochemistry University of Maryland, at Baltimore,MD, Dept of Physics, University of Illinois at Urbana, IL Dept. of Chemistry, University of Gdansk, Gdansk, Poland .

Our recent linear dichroism study indicate that heme is not a planar oscillator when it acts as an acceptor of radiationless excitation energy transfer from tryptophan . The linear nature of the heme absorption transition moment in the near UV region implies a strong dependence of the transfer rate factors on the relative angular position of heme and tryptophan, i.e. on the κ^2 orientation parameter of the Förster equation. Using the atomic coordinates of human hemoglobin and taking into account the direction of the transition moment of the near UV (300-380 nm) heme absorption band we have estimated the rate of energy transfer from tryptophan to heme in the isolated α chains, which are a single tryptophan protein. On this basis we were able to predict very accurately the two lifetimes detectable in the systems, of 31 and 1050 ps respectively, where the amplitude of the longer lifetime is very consistent with the amount of disordered hemes found by La Mar et al.,(1983, J. Mol. Biol., **168**, 887; 1984, J. Am. Chem. Soc. **106**, 6395) for the α subunits of hemoglobin. The long lifetime decreased to 650 ps at high protein concentration (30 mg/ml) consistent with the formation of dimers, where, normal hemes quench at intersubunit distance the tryptophan fluorescence only partially quenched by disordered hemes at intrasubunit distance. The excellent consistence between simulated and measured values suggests that the isolated α subunits of hemoglobin conserve the tertiary and quaternary structure they have in tetrameric hemoglobin.

M-AM-E6

Origin of the short and long lifetimes of human hemoglobin.
Zygmunt Gryczynski, Jacek Lubkowski, Enrico Gratton, and Enrico Bucci. Dept of Biochemistry, Univ. of Maryland at Baltimore,MD, Dept. of Chemistry, Univ. of Gdansk,Poland.

We measured the time resolved fluorescence of human oxy- and deoxy-hemoglobin in 30 mM either phosphate or borate buffer at pH 6.6 and 9 respectively. In all cases the intensity decay showed the presence of two discrete lifetimes one near 30 ps and 800 ps respectively. We compared our data with computation based on the atomic coordinates of human oxy- and deoxy-hemoglobin, and the Förster theory of radiationless excitation energy transfer. It was possible to infer that the shorter lifetimes originated from the quenching of tryptophans by hemes at intrasubunit distances, which decreased 60-70 times the emission of tryptophan. The crystal coordinates also indicated that the longer lifetimes were due to a much lower quenching produced by disordered hemes, i.e. rotated 180° around their α-γ meso-axis. This reduced the intensity of tryptophan emission only 2-3 times. Notably, the atomic coordinates indicated that only the α chains were sensitive to the presence of disordered hemes. La Mar [(1983, J. Mol. Biol., **168**, 887; 1984, J. Am. Chem. Soc. **106**, 6395)] has shown that in liganded hemoglobin 2 % of the α subunits carry a disordered heme. Consistent with these observation the amplitudes of the long lifetimes were 2% of the total. In deoxyhemoglobin the amplitude of the long lifetimes decreased to 0.5 % suggesting a lower fraction of disordered hemes in the system. This phenomenon was reversible with oxygenation.

M-AM-E7

STABILITY OF HbXL99α UNDER HIGH PRESSURE: AN INTRINSIC FLUORESCENCE STUDY.
((R.E. Hirsch[a], J.M. Friedman[a], J.P. Harrington[b], and S.F. Scarlata[c].)) [a]Albert Einstein College of Medicine, Bronx, NY, [b]University of South Alabama, Mobile, AL, [c]SUNY Medical Center, Stony Brook, NY.

One important criteria for a plasma circulating hemoglobin blood substitute is resistance to subunit dissociation. For this reason, cross-linked hemoglobins (with low oxygen affinities) are being specifically designed to serve as potential blood substitutes. An example is HbXL99α which is cross-linked between the α-subunits [PNAS (1987) 84:7280]. It has been previously shown that hemoglobin dimerization results in alterations of the intrinsic fluorescence [BBRC (1983) 116:712; Anal. Biochem. (1985) 149:415]. In the study presented here, the effects of up to 2 kilobars of pressure on the intrinsic fluorescence of the cross-linked HbXL99α, HbA, and myoglobin were examined and compared. Hemoglobin solutions were studied between 0.01 - 0.1g% in potassium phosphate or Hepes buffers, pH 7.4. Results show HbA exhibits a decrease in fluorescence intensity as a function of pressure. In contrast, HbXL99α as well myoglobin (a monomer) show only a small change in intrinsic fluorescence intensity (~9%) as a function of pressure. These results suggest that HbXL99α is stable as a tetramer up to ~2 kilobars of pressure. In addition, high pressure spectroscopic studies provide a suitable technique for determining the subunit stability of cross-linked or polymerized hemoglobin and hemoglobin derived blood substitutes.

M-AM-E8

LIGAND POCKET CONFORMATION OF PARTIALLY LIGANDED HEMOGLOBIN PROBED BY EPR.
((J.M. Rifkind, P.T. Manoharan, and O. Abugo)) NIH/NIA Gerontology Research Center, Baltimore, MD 21224 and Indian Institute of Technology, Madras 600 036, India

Electron paramagnetic resonance (EPR) does not detect reduced Fe^{2+} hemoglobin, but is particularly sensitive to the heme environment of oxidized Fe^{3+} hemoglobin. We have previously shown that the Fe^{3+} EPR spectrum is influenced by the quaternary conformation of the hemoglobin.[1] Oxidized subunits are considered to be in the liganded conformation. We have therefore used three methods to prepare partially liganded hemoglobin: 1) the level of oxidation was varied; 2) the oxygenation of the Fe^{2+} chains were varied while the EPR spectrum of the Fe^{3+} chains was analyzed; 3) the valence hybrids $(\alpha'\beta)_2$, $(\alpha\beta')_2$ and $(\alpha'\beta')(\alpha\beta)$ were prepared and their EPR spectra analyzed. From the spectra, changes in the geometry of both the high-spin and low-spin aqueous complexes were detected. Alterations in ligand pocket dynamics were also demonstrated by the redistribution of substates that takes place during incubation at 235 K. These results provide information regarding the conformation of monoliganded hemoglobins and the various biliganded hemoglobins. Evidence is presented for distinct conformations of the various partially liganded hemoglobins.

[1] A. Levy, V.S. Sharma, L. Zhang and J.M. Rifkind, Biophysical Journal 61, 750-755 (1992).

M-AM-E9

CORRELATION OF ELECTRIC FIELD AND VIBRONIC SPECTRAL SHIFTS IN CYTOCHROME *c* PEROXIDASE: EFFECT OF SOLVENT AND BINDING OF CYTOCHROME *c*.

((H. Anni, K.A. Sharp, T. Yonetani, J. Fidy and J.M. Vanderkooi))
University of Pennsylvania, Department of Biochemistry & Biophysics, Philadelphia, PA 19104-6089.

Vibrationally-resolved optical absorption spectra of mesoporphyrin-substituted cytochrome *c* peroxidase (MP-CcP) were measured at 5 K by fluorescence line narrowing (FLN), as a function of solvent parameters and binding of ferrous cytochrome *c* (cyt *c*). The electric field that CcP imposes at its heme was calculated at different ionic strengths. The pH effect on the electric field was considered as changes in the protonation state of Glu, Asp, Arg, Lys, His and heme propionates of CcP. We found that depending on pH, two to three components contribute to the FLN spectrum of MP-CcP. They represent either phototautomers of MP or their conformers. The experimentally-determined frequencies of the 0,0 transitions for these components were not altered by ionic strength of the solvent. In parallel, our calculations showed that the electric field at the heme is insensitive to changes of ionic strength. One component was shifted at alkaline pH due to either the unprotonation of distal His52 or breaking of the hydrogen-bonding of MP to proximal His175. Accordingly, an increase of the electric field of CcP at the heme was calculated for charging His52 and His175. In the cases of ionic strength and pH, there is a clear correlation of spectral shifts and electric field. Since binding of cyt *c* produced no shifting of the 0,0 frequencies of MP-CcP components, we predict that in the presence of cyt *c* the electric field at the neighboring heme of CcP is not affected. (Supported by NIH P01-GM48130)

M-AM-E10

Temperature dependence of the Fe^{2+}–N_ϵ (His F8) Raman–band of deoxyMyoglobin ((H. Gilch, W. Dreybrodt and R. Schweitzer-Stenner))
Institute of Exp. Physics, University of Bremen, 28359 Bremen, Germany

The broad Raman profile resulting from the ν_{Fe-His} stretching mode in *horse heart* deoxyMb can be resolved into three sublines (SL) with temperature independent frequencies $\Omega_1 = 208\ cm^{-1}$, $\Omega_2 = 216\ cm^{-1}$ and $\Omega_3 = 225\ cm^{-1}$. We have measured the area of these SL at temperatures from 300 to 10 K. The intensity ratio I_3/I_2 exhibits a van't Hoff behaviour between 300 K and 150 K, bending over in a region between 150 K and 80 K and then remains constant. The ratio I_2/I_1, however, shows a maximum at $T \approx 170$ K and approaches a constant value at 80 K. The data can be fitted by a van't Hoff expression, taking into accout the linear temperature dependence of the specific heat of proteins. This leads to temperature dependent changes of entropy and enthalpy upon conformational interconversion between the conformers attributed to each line. From the thermodynamic data, the freezing temperature $T_f = 120$ K and the width of the transition region $\Delta T = 55$ K, we conclude that the conformational substates (CS) are related to fluctuations of the protein at the proximal side of the heme pocket. In comparison we have evaluated the temperature dependence of the ratios A_0/A_1 exhibited by the SLs due to CS of the CO-stretch in MbCO (Ansari et al., Biophys. Chem., 26, 337, 1987). All thermodynamic parameters are larger by one order of magnitude, $T_f = 240$ K, $\Delta T = 5$ K. This resembles the properties of protein bound water. We thus conclude that the fluctuations of the tight compartment formed by the distal side of the heme pocket are driven by those of bound water.

STRUCTURE AND FUNCTION OF THE FIRST ENERGY COUPLING SITE

M-AM-SymII-1

Structural Analysis of Mitochondrial Complex I.
John E. Walker, MRC Lab. of Molecular Biology, Cambridge, U.K.

M-AM-SymII-2

THE USE OF MOLECULAR GENETICS TO STUDY THE RESPIRATORY COMPLEX I IN *NEUROSPORA CRASSA* AND *ESCHERICHIA COLI*

((H. Weiss, T. Friedrich, H. Leif, W. Fecke, A. Berger, C. Krüll and M. Braun)) Universität Düsseldorf, Institut für Biochemie

NADH:ubiquinone oxidoreductase (complex I) of mitochondria and bacteria links electron transfer from NADH to ubiquinone with proton translocation. One FMN and 7-8 iron-sulphur clusters serve as prosthetic groups in this reaction. The mitochondrial complex contains some 40 different subunits, of which the seven most hydrophobic subunits are encoded by genes on the mtDNA. The *E. coli* complex I contains 14 subunits for all of which homologuous counterparts are found in the mitochondrial complex I. Among them are all subunits predicted from sequences to bind the substrates and the redox groups, as well as all 7 mitochondrially encoded subunits. The genes of the *E. coli* complex I are organized as one operon. The gene order reflects the topological arrangement of the subunits. Genes of the peripheral subunits cluster together as do genes of the membrane intrinsic subunits. By gene disruption in *N. crassa* the mitochondrial complex I can be dissected *in vivo*. Preassembled parts are accumulated and can be characterized. In *E. coli* the structure function relationship of complex I subunits is studied by site directed mutagenesis.
Nehls et al. (1992) J. Mol. Biol. 227, 1032-1042.
Weidner et al. (1993) J. Mol. Biol. 233, 109-122.

M-AM-SymII-3

EPR STUDIES OF STRUCTURE-FUNCTION RELATIONSHIPS IN THE MITOCHONDRIAL AND BACTERIAL NADH-Q OXIDOREDUCTASES
((Tomoko Ohnishi, V.D. Sled*, T. Yano*, T. Yagi*, Y. Hatefi*, T. Friedrich+, H. Leif+, W. Fecke+, H. Weiss+)) Univ. of Pennsylvania, Philadelphia, PA 19104, *Dept. Molec. & Exptl. Med., The Scripps Res. Inst., La Jolla, CA 92037,+Inst. of Biochem., Univ. of Düsseldorf, 4000 Düsseldorf 1, Germany.

Previous analyses of mitochondrial NADH-Q oxidoreductase (Complex I) indicated non-covalently bound FMN, two binuclear clusters, and four tetranuclear clusters as intrinsic redox centers. Comparison of the primary sequence of mitochondrial Complex I subunits and its counterparts (NDH-1) in various bacteria has predicted that 5 subunits with molecular weights of 75, 51, 24, 23, and 20 kDa harbor 7-8 clusters, based on conserved sequence motifs. EPR identification of individual iron-sulfur clusters and their subunit location have been greatly facilitated by the following molecular genetic approaches: (1) Inactivation of specific genes of *Neurospora crassa* Complex I and *Escherichia coli* NDH-1 by the homologous replacement with a defective gene copy. (2) Overexpression of individual subunits of *Paracoccus denitrificans* in *E. coli*, and their purification. (3) Site-directed mutagenesis of putative ligand residues in *E. coli*. We have also analyzed the thermodynamic and EPR profile of the flavin as a converter of the n=2↔n=1 electron transfer step, and its direct interaction with ferricyanide in the free radical state, using isolated Complex I [supported by NIH GM-30736 (T.O.), GM-33712 (T.Y.), DK-08126 (Y.H.), and Deutsche Fors. Gem. (H.W.)].

M-AM-SymII-4

MECHANISM AND REGULATION OF THE MAMMALIAN NADH-UBIQUINONE OXIDOREDUCTASE.

((A. D. Vinogradov)) Department of Biochemistry, School of Biology, Moscow State University, Russia.

In contrast to intact Complex I the resolved three-subunit NADH-dehydrogenase shows dramatic difference in the protein affinity to the reduced or oxidized flavin. This finding is taken as an indication of possible intramolecular dislocation of the flavin during catalysis and its involvement in the vectorial loop mechanism of proton translocation ($2H^+/2e$) at the coupling sub-site between NADH and center N-2. The vectorial dismutation of two protonated (from the matrix side) ubisemiquinones magnetically interacting with N-2, which results in release of $1H^+/2e$ on cytosolic side, is proposed as a mechanistic model for the coupled oxidoreduction between center N-2 and bulk ubiquinone. Operating together two coupling sub-sites give the overall stoichiometry of $3H^+/2e$. Complex I within the inner mitochondrial membrane is the subject of the slow oxidoreduction dependent active/inactive transition which results in a futile cycling. The fraction of active Complex I is under control of a number of parameters (Q/QH_2 ratio, divalent cations, pH) and may play an important role in the enzyme regulation.

M-AM-F1

THREE-DIMENSIONAL STRUCTURE OF RAT LIVER 3α-HYDROXYSTEROID DEHYDROGENASE/DIHYDRODIOL DEHYDROGENASE: A MEMBER OF THE ALDO-KETO REDUCTASE SUPERFAMILY ((Hoog, S.S.[1], Pawlowski, J.E.[2], Alzari, P.M.[3], Penning, T.M.[2], and Lewis, M.[1])) [1]Dept. Biochem & Biophysics [2]Dept. Pharmacology University of Pennsylvania Medical School,Philadelphia, PA 19104 [3] Institut Pasteur, Paris, France (Spon. by T. Sosnick)

The 3.0 Å resolution x-ray structure of rat liver 3α-hydroxysteroid dehydrogenase/dihydrodiol dehydrogenase (3α-HSD,EC 1.1.1.50) was determined by molecular replacement using human placental aldose reductase as the search model. The protein folds into an α/β or triosephosphate isomerase (TIM) barrel and lacks a canonical Rossman fold for binding pyridine nucleotide. This is the first structure of a mammalian hydroxysteroid dehydrogenase. The structure contains a concentration of hydrophobic amino acids that lie in a cavity near the top of the barrel which are presumed to be involved in binding hydrophobic substrates (steroids, prostaglandins and polycyclic aromatic hydrocarbons). At the distal end of this cavity lie three residues in close proximity that have been implicated in catalysis by site directed mutagenesis--Tyr 55 Asp 50 and Lys 84. Tyr 55 is postulated to act as the general acid. 3α-HSD shares significant sequence identity with other HSDs that belong to the aldo-keto reductase superfamily and these may show similar architecture. Prostaglandin F synthase and rho-crystallin are also members of this family. By contrast, 3α-HSD shares no sequence identity with HSDs that are members of the short chain alcohol dehydrogenase (SCAD) family, but does contain the Tyr X X X Lys consensus sequence implicated in catalysis in this family. In the 3α-HSD structure these residues are on the periphery of the barrel and are unlikely to participate in catalysis.

M-AM-F2

Entropy changes in biological processes: Side chain entropy losses in folding and binding.

K. H. Lee†*, D. Xie*, E. Freire* and L. M. Amzel†. †Department of Biophysics and Biophysical Chemistry, School of Medicine, *Department of Biology, and *Department of Physics and Astronomy, Johns Hopkins University, Baltimore, Maryland 21205

Estimation of free-energies of folding and binding requires an accurate evaluation of both enthalpic and entropic contributions to the processes. One major component of the entropic terms involves the loss of configurational entropy by some of the side chains. The entropy of side chains in proteins can be accurately estimated using statistical mechanical methods. We have estimated the entropies of most amino acid side chains in a helical environment. The calculations were performed under several different sets of assumptions each suited for the estimation of the entropy loss in a different process. The side chain entropy loss during a binding or folding process, when a side chain in a folded protein goes from being exposed to being burried can be estimated completely using statistical mechanical methods. The entropy loss of the side chains during folding was estimated after subtracting the estimated enthalpy from the free-energy of folding in systems involving single amino acid substitutions that resulted in proteins of different stability. The methods used provide a reliable way of estimating the side chain entropy losses in processes involving transitions from random-coil to folded-exposed and folded-exposed to folded-burried. This work was supported by grants RR04328, GM37911, GM44692, and NS24520

M-AM-F3

SIDE CHAIN ENTROPY AND PACKING IN PROTEINS.
((Sarina Bromberg & Ken A. Dill)) Dept. Pharm. Chem., Box 1204 UCSF, CA 94143-1204.
What role does side chain packing play in protein stability and structure? We compare a lattice model with side chains (SCM) to a linear lattice model without side chains (LCM). Self-avoiding configurations are enumerated in 2 and 3 dimensions (D) exhaustively for short chains and by Monte Carlo sampling for chains up to 50 backbone monomers long. The SCM lacks any specific jigsaw puzzle packing among side chains that might discriminate one native fold from another, but this model nonetheless demonstrates the importance of side chain packing: (1) Side chain degrees of freedom increase the entropy of open conformations, but side chain steric exclusion decreases the entropy of compact SCM conformations, thus producing a substantial entropy that opposes folding. (2) There is a side chain "freezing" or ordering, *i.e.*, a sharp decrease in entropy, near maximum compactness. (3) The different types of contacts among side chains (*s*) and main chain (*m*) have different frequencies, and different dependencies on compactness. *mm* contacts contribute significantly only at high densities, suggesting that backbone hydrogen bonding in proteins may be promoted by compactness. The distributions of *mm*, *ms* and *ss* contacts in compact SCM configurations are similar to the distributions in protein structures in the Brookhaven Protein Data Bank. We suggest that packing in proteins is more like the packing of nuts and bolts in a jar than like the pairwise matching of jigsaw puzzle pieces.

M-AM-F4

THE VOLUME CHANGE OF COFACTOR BINDING TO DEHYDROGENASES. ((V.D. Daggett, K. Kirshenbaum, J.K. Pedersen, and P.C. Kahn)) Dep't of Biochemistry & Microbiology, Rutgers Univ., New Brunswick, NJ 08903. (Spon. by M. Takahashi)

Horse liver alcohol dehydrogenase (HLADH) binds its co-factor NAD+ or NADH in a large open cleft, which closes down upon the ligand like a clam, shielding it from contact with the solvent. The binding is entropy driven, the favorable free energy arising from the expulsion of water of solvation. In contrast, yeast alcohol dehydrogenase and glutamate dehydrogenase bind the same co-factor in a small cleft which does not close. These reactions are enthalpy driven, their entropies being unfavorable. The amount of water expelled from the biomolecular surfaces is insufficient for its rise in entropy to offset the unfavorable contributions. The density of hydrating water also differs from bulk solvent. Expulsion into the surrounding milieu therefore entails a change in volume. We have measured ΔV of co-factor binding to all three enzymes, finding +85 ml/mole of ligand bound for association of either NAD+ or NADH with HLADH and zero for the other two. This requires that the solvent density within the hydration zones exceed 1 g/ml. Were the averaged density within these zones to be 1% greater than that of the bulk, a ΔV of 85 ml/mole would entail the expulsion of some 470 water molecules. Calculations of the change in solvent accessible surface area from crystal structures of the liganded and unliganded forms allow estimates of the density and thickness of the averaged "layer" of hydration.

M-AM-F5

PF4 ALCOHOL-INDUCED PROTEIN FOLDING INTERMEDIATES AND TRANSITIONS: THE O-STATE.
((K.H. Mayo, Yingqing Yang, Elena Ilyina)) University of Minnesota, UMHC, Box 609, Minneapolis, MN 55455.

Titration of platelet factor-4 (PF4) with low molecular weight, aliphatic alcohols, induces reversible protein folding transitions which are observed to be in slow-intermediate exchange on the 600 MHz ^{1}H-NMR chemical shift time scale. The alcohol-induced state is called the O-state. O-state/N-state folding exchange rates occur on the 1-100 millisecond time scale depending on alcohol concentration. NMR spectra suggest that the O-state has a more "unfolded" structure, while CD data indicate the preservation of considerable secondary structure. Increasing alcohol concentrations shifts CD-derived fractional compositions significantly with overall β-structure decreasing by about 20% and α-helix composition increasing by about 25%. NMR alcohol-jump experiments indicate folding reversibility and conservation of about 15 long-lived NHs in native and O-states which can be assigned to residues in anti-parallel β-sheet structure. Overall, the PF4 O-state is a stable intermediate with an apparently more highly fluctuating anti-parallel β-sheet domain and a more stabilized C-terminal α-helix.

This project has been supported by NIH Research Grant HL43194.

M-AM-F6

THE EFFECT OF A TYR → GLU MUTATION ON THE THERMODYNAMICS OF HETEROLOGOUS AND HOMOLOGOUS ASSOCIATION OF LIGHT AND HEAVY DOMAINS OF THE HUMANIZED 4D5 ANTI-p185^{HER2} ANTIBODY. ((Jeff R. Livingstone, Steven J. Shire† and Robert F. Kelley‡)) FCRDC, NCI, Frederick, MD 21702 and Departments of ‡Protein Engineering and †Pharmaceutical Research and Development, Genentech, Inc., 460 Pt. San Bruno Blvd., South San Francisco, CA 94080

Antibody IgG variable fragments (FV) are comprised of one light (VL) and one heavy (VH) domain held tightly together by noncovalent interactions (hydrogen bonds, hydrophobic interactions). We have investigated the thermodynamics of heterologous domain-domain association in the humanized 4D5 anti-p185^{HER2} antibody FV as well as homologous association of individually purified VL and VH domains by sedimentation equilibrium (SE), isothermal titration calorimetry (ITC), and polarization anisotropy (PA). Association constants (K_2) and heats of association (ΔH_2) for VL and VH dimer formation were determined by SE. These values, in concert with equilibrium constants (K_a) and heats of heterologous association (ΔH_a) determined by PA and ITC, create a complete thermodynamic profile of the coupled equilibria that occur between VH and VL domains in solution. In conjunction with recent antibody structural data, this work provides the beginning of a structure-function framework for understanding how protein engineering efforts (*e.g.* humanization, creation of bi-specific antibodies) effect antibody stability. As a specific example, we demonstrate here the consequences of a single tyrosine to glutamate change at position 55 in VL on the entire thermodynamic profile of the heterologous association of FV and homologous association of VL.

M-AM-F7

EFFECTS OF MUTAGENESIS ON THE N-CAPPING BOX OF HGH HELIX #2.

((E.A. Zhukovsky, M.G. Mulkerrin, and L.G. Presta))
Depts of Protein Engineering and Medicinal and Analytical Chemistry, Genentech, Inc., South San Francisco CA 94080. (Spon. by M.G. Mulkerrin)

One of the most intriguing problems in structural biochemistry is the determination of the stereochemical code which defines conformational specificity and governs protein folding. In this study we have attempted to evaluate, using human growth hormone (hGH) as our model compound, the importance of helix caps (N-capping box) and charge-dipole interaction on helix formation and stability.

At the N-terminus of helix #2 of hGH there are two residues, Ser 71 and Glu 74, which form an N-capping box. In order to evaluate the stabilizing effect of the negative charge and of each hydrogen bond we used site-directed mutagenesis. We used spectroscopic, binding and GuHCl protein denaturation assays to monitor changes produced by the point-mutations.

The results of these experiments can be summarized as follows: *a*) binding and spectroscopic assays suggest that the secondary and the tertiary conformations of the mutants are similar to that of the *wt*, *b*) either H-bond of the N-cap has more pronounced effect on stability of the hGH than the negative charge at position #74, *c*) the H-bond formed by the side chain of the N-cap residue (#71) has a larger stabilizing effect than the *N*+3 residue (#74), *d*) mutant stability is not sensitive to the nature of the residue occupying the cap position as long as its H-bonding capacity is eliminated, and *e*) the charge-dipole interaction shows minimal stabilization effect in the absence of H-bonding capacity of the residue at position #74.

M-AM-F8

THE EFFECT OF N-TERMINAL ACETYLATION ON THE STRUCTURE OF A N-TERMINAL TROPOMYOSIN PEPTIDE.

((N.J. Greenfield[1], W.F. Stafford[2] and S.E. Hitchcock-DeGregori[1])) [1]UMDNJ-Robert Wood Johnson Med. Sch., Piscataway, NJ 08854 and [2]Boston Biomed. Res. Inst., Boston, MA 02114.

Tropomyosin is N-terminally acetylated in vivo and the acetyl group is required for normal actin binding. We have used a peptide consisting of the first 30 residues of striated muscle α-tropomyosin, with GlyCys added to the C-terminus, to determine the effect of N-terminal acetylation on the conformation and stability of the N-terminal domain of tropomyosin. Under physiological conditions the 32mer was mainly disordered, and disulfide cross-linking or N-terminal acetylation had little effect on its conformation. Addition of salt, however, induced the formation of α-helix. In high salt (> 1 M), the CD spectrum, the cooperativity of folding, and sedimentation equilibrium ultracentrifugation of the peptide showed that it formed a two-chained coiled-coil α-helix. In high salt, disulfide cross-linking and N-terminal acetylation stabilized coiled coil formation in a synergistic fashion. Addition of 50% trifluoroethanol or 40% ethanol to the peptide also increased its α-helical content, but the CD spectra and unfolding behavior of the 32mer showed no evidence of coiled coil formation. Moreover, N-terminal acetylation had very little effect on the conformation or stability of the peptide under these conditions. The results show that N-terminal acetylation stabilizes the coiled-coil conformation. The effect probably cannot be explained by interactions with the "helix-dipole" since the stabilization is observed in very high salt. Supported by NIH and MDA.

M-AM-F9

ENERGETICS OF MOLTEN GLOBULE STATE OF APOMYOGLOBIN.

((Yu.V.Griko and P.L. Privalov)) Department of Biology, The Johns Hopkins University, Baltimore, MD 21218

Stability of apomyoglobin in the molten globule state and its temperature induced transition into an unfolded state has been studied by scanning microcalorimetry, CD spectroscopy, and viscometry. It has been shown that a compact, partly unfolded state of apomyoglobin, which is obtained in acidic solutions, has a heat capacity lower than that of the unfolded polypeptide chain. With increasing temperature, this intermediate state unfolds in a rather narrow temperature region. Its unfolding is accompanied by an increase of the heat capacity which reaches the value specific for the fully unfolded polypeptide chain having all groups exposed to solvent. This unfolding, however, proceeds without the excess heat absorption expected for a temperature induced two-state transition. This eliminates possibility of considering this process as a first order phase transition, as gross conformational transitions in proteins are usually considered. It appears that the process of the unfolding of the intermediate state of myoglobin might represent a second order phase transition, which has been predicted on theoretical grounds for the compact proteins without unique structure, known as "molten globules".

THEORY I

M-AM-G1

UNITARY AND BINARY COMPACT DOMAINS IN PROTEINS

((M.H. Zehfus)) College of Pharmacy, The Ohio State University, Columbus, OH, 43026

Compactness may be quantified using a normalized measure of surface area. While compactness has been used already to identify continuous protein domains, the calculations were too time consuming to be used to find discontinuous domains containing two or more polypeptide chains.

Using a new look-up table based algorithm for calculating surface area and volume, it is now possible to exhaustively calculate the compactness of all potential substructures containing either one or two polypeptide chains. This methodology has been applied to several well characterized proteins (BPTI, ribonuclease, cytochrome *c*, myoglobin, T4 lysozyme and interleukin 1β) to identify the unitary and binary compact domains in these proteins.

In general, binary units with two peptide chains are more compact and more numerous that the unitary units with a single peptide chain. For each protein two or three compact units may be found that span most of the protein's sequence, have little mutual overlap, and have optimal compactness. These units are proposed to be the protein's primary domains. Experimental evidence on domain structure seems to agree well with these proposed domains.

M-AM-G2

AN INTEGRATED APPROACH TO MODELING MACROMOLECULAR ELECTROSTATICS.

((H. Oberoi & N. M. Allewell)) Department of Biochemistry, University of Minnesota, St Paul, MN 55108.

Electrostatic interactions in proteins have been modeled extensively with various forms of the Poisson-Boltzmann equation and a semi-macroscopic representation of the molecule and solvent. The multigrid method allows rapid solution of the nonlinear Poisson-Boltzmann equation and allows titration curves and potentials to be calculated for significantly larger proteins than possible previously [Oberoi & Allewell, Biophys. J. 65:48 (1993)]. We have developed an integrated package (TiNy) that applies concepts from object oriented programming and shell languages to provide an interface that is intuitive and flexible. The program is highly modular and easily extendable. High level functions for manipulation and display of macromolecules, and their charges and potentials are provided. We have used TiNy to calculate titration curves for lysozyme, ribonuclease A, human thioredoxin and free energies of assembly and ligand binding for aspartate transcarbamylase. Root mean square differences in experimental and calculated pK values are on the order of 1 pH unit for lysozyme. The degree of agreement depends critically on the resolution of the structure, particularly sidechain positions, and on the atoms to which titrating charges are assigned.

Supported by NIH grant DK-17335 (to NMA)

M-AM-G3

EXPERIMENTAL AND THEORETICAL STUDIES OF PRION PROTEIN STRUCTURES.
((Z. Huang, J.-M. Gabriel, K.-M. Pan, M. Baldwin, J. Nguyen, R. J. Fletterick, S. B. Prusiner and F. E. Cohen)) Departments of Pharmaceutical Chemistry, Neurology, Biophysics and Biochemistry, and Medicine, University of California, San Francisco, CA 94143-0446. (Spon. by F. E. Cohen)

The prion protein is responsible for prion diseases, a group of neurodegenerative disorders including Creutzfeldt-Jakob disease and Gerstmann-Straussler-Scheinker syndrome in humans, and scrapie and bovine spongiform encephalopathy in animals. We purified the prion protein in both the normal cellular form and abnormal diseased form and determined the secondary structure of each using spectroscopic experiments. We found that the cellular form and diseased form of the prion protein may differ from each other only in their conformations, with the cellular form of the protein containing predominantly α-helices while the diseased form shows a high β-sheet content. This suggested that prion diseases could be a result of conformational changes of the prion protein. Applying various secondary and tertiary structure prediction methods, we carried out theoretical computational study to determine the three-dimensional structures of the prion protein. The predicted structures provide valuable insight into the molecular mechanism of prion diseases, rationalize much of the mutational data correlated with the genetic forms of prion diseases, and guide further structural studies of important peptide fragments of the prion protein using NMR spectroscopy and molecular dynamics simulations.

M-AM-G4

HELIX FOLDING SIMULATIONS AND THE MULTIPLE-MINIMA PROBLEM
((Shen-Shu Sung)) Research Institute, Cleveland Clinic Foundation, Cleveland OH 44195

The multiple-minima problem is a well known obstacle in searching for the global minimum-energy conformation of proteins. This presentation reports helix folding simulations at normal temperatures that do not suffer from the multiple-minima problem. Starting with different conformations, including the fully extended conformation, the randomly generated conformation, the conformation with β-sheet hydrogen bonds, and the left-handed helix, the 16-residue alanine-based peptides folded into predominantly right-handed α-helical conformations during constant temperature (274°K) simulations without using thermal perturbations. The rigid-element method (S.-S. Sung, Biophys. J. 1993, 64:A245) and the AMBER force field were used in the simulation. The efficiency of the method, the temperature factor, and a proper reference of energy are the key factors for the success. Interesting insights into the helix folding mechanism were revealed. The electrostatic interactions between the successive amides favor extended conformations (or β strands) and cause energy barriers for helix folding. The β-bend intermediates were observed during the helix nucleation. The helix propagation toward the C-terminus seemed more probable than that toward the N-terminus for the homopolymer of alanine. The hydrogen bonds in helical conformations frequently oscillated between the (i,i+4) and the (i,i+3) patterns. The (i,i+3) hydrogen bonds occurred more frequently during the helix propagation and deformation near both ends of the helical segments.

M-AM-G5

MOLECULAR DYNAMICS SIMULATIONS OF SALMON AND HUMAN CALCITONINS IN AQUEOUS SOLUTION.
((R. Osman and A. Smolyar)) Department of Physiology and Biophysics, Mount Sinai School of Medicine, CUNY, New York, NY 10029.

The structures of a salmon (sCT) and human (hCT) calcitonins, 32 aminoacids peptides, were constructed based on a structure deduced from 2D-NMR of sCT in dodecyl sulfate micelles. The peptides were placed in a rectangular box filled with pre-equilibrated water. The dimensions of the box were defined by a distance of at least 8 Å from any atom of the peptide. The structure of water was minimized while the peptide was kept frozen followed by a minimization of the complete system. The systems were heated to 300K over 10 ps, followed by 90 ps of constant temperature molecular dynamics (MD) simulation. During this time the temperatures of the solvent and the solute were adjusted by changing the individual coupling constants to the bath. At the end of the equilibration period, additional 100 ps of constant temperature simulations were carried out. Periodic boundary conditions were used throughout. Analysis of the averaged structures and the MD trajectories of the last 100 ps from both simulations shows that helix that connects a cyclic loop between Cys^{1} and Cys^{7}, with a β-turn at the C-terminus is different in the two peptides. An examination of the torsional angles of the backbone reveals that the helix in sCT starts with Lys^{11} and persists through Thr^{25} with some perturbation around Gly^{20}. In the hCT the helix starts only at Tyr^{12} and ends at Gln^{24}. An analysis of the water structure around the begining and the end of the helices provides a possible explanation for the unwinding of the ends of the helix in hCT. The specific role of different amino acids residues in helix stabilization results from their ability to prevent water penetration to disrupt the helical hydrogen bonds.

M-AM-G6

KINETICS OF NONSTATIONARY, DIFFUSION-INFLUENCED REVERSIBLE REACTIONS IN ONE DIMENSION.
(H. Martinez) Institute of Theoretical Dynamics, University of California, Davis, CA 95616

There are many physical-chemical processes whose kinetics are influenced by diffusion, such as enzyme-substrate reactions. Clearly, these processes are of significant practical importance and it is desirable to have a theoretical framework providing an unambiguous understanding of these phenomena. The statistical nonequilibrium thermodynamic theory of diffusion-influenced reactions is extended to non-stationary situations. Coupled dynamic equations for the average concentrations and the radial distribution function are derived, and, in the low density limit, applied to study the approach of the reversible reaction to equilibrium. The influence of a constant external field is also studied. The presence of the external field delays the approach to the asymptotic behavior.
This study in one dimension is meant to shed some initial light on the theoretical understanding of anomalous processes taking place in more complex systems.

M-AM-G7

CONSTRAINTS IN BIOCHEMICAL REACTIONS.
((R. A. Alberty)) MIT, Cambridge, MA 02139

Chemical reactions satisfy element and charge conservation equations, but generally do not satisfy additional independent conservation equations. Biochemical reactions at a specified pH satisfy conservation equations for elements in addition to hydrogen, but they often satisfy additional independent conservation equations because of the coupling of reactions through the enzymatic mechanism. The enzyme may couple together two or more biochemical reactions so that only the sum of the coupled reactions is catalyzed. The biochemical reactions that are coupled together may, or may not, share reactants, but the type of coupling discussed here is stoichiometric. Since chemical equations and biochemical equations are mathematical equations, linear algebra provides the means for determining the number and types of constraints involved in the enzymatic mechanism. Constraints in addition to element balances indicate missing reactions. The identification of conservation equations is essential for calculations of equilibrium compositions using computer programs that minimize the transformed Gibbs energy at a specified pH subject to the conservation equations that apply.

M-AM-G8

MESOSCOPIC THEORIES FOR PROTEIN CRYSTAL GROWTH.
((J.G.E.M. Fraaije, J.T.W.M. Tissen, J. Drenth and H.J.C. Berendsen)) RUG, Nijenborgh 4, 9747 AG Groningen, The Netherlands.

A computer simulation method is proposed to study the hydrodynamic interactions of protein molecules. The central idea is that the only force acting over a lengthscale comparable with the size of the protein molecules is the hydrodynamic interaction. This is very important when considering steering effects in the process of nucleation. The Stokes equations of motion for the protein molecules, the creeping flow (Navier-Stokes) equations for the solvent together with the no-slip boundary conditions give a complete representation of the system. The resulting 3-D boundary value problem can be rewritten in a 2-D form considering the discretized surfaces of the particles only. By solving the equations on the surface elements the so-called mobility matrix is determined. All hydrodynamic interactions are included in this matrix. After calculation of the conservative forces and the stochastic force (due to collisions with the solvent molecules) the new translational and rotational velocities of the protein molecules can then be determined. The simulation method can be applied to arbitrary particle shapes. It can also handle arbitrary flow fields, and the effects of applying a flow field (convection?) to the system can be studied. From analysis of the trajectories information can be gained on the kinetics and thermodynamics in the early stages of the crystallization process.

M-AM-G9

DIFFUSION OF SOLUTES THROUGH BIOMEMBRANES: ATOMIC-LEVEL MOLECULAR DYNAMICS SIMULATIONS

((T.R.Stouch, D.Bassolino, H.Alper)) Bristol-Myers Squibb Pharmaceutical Research Institute, Princeton, NJ 08543-4000

Atomic-level molecular dynamics simulations were used to study the process of the penetration of membranes by small molecules with the goal of predicting transport of drugs through biomembranes. Excellent agreement with experiment was found for structural and dynamical properties of both the diffusion of small molecules as well as the response of the membrane to those solutes. The simulations further agree with experiment and high-level theory that indicate that biological membranes have a gradient of structure that influences the permeation process. The gradient of structure stands in contrast to the assumption that the membrane/water interface is well-represented by the octanol/water interface. Penetration of the charged lipid headgroup region was found to be the rate-determining step of the diffusional process. In part, small solutes were found to diffuse by hopping motions between voids within the lipid bilayer of the membrane. This mechanism varies, dependant on location in the membrane and size of the solute.

NEURONAL CALCIUM CHANNELS

M-AM-H1

INTERACTION OF ω-AGA-IVA AND ω-CONOTOXIN MVIIC WITH THE 5-HT SENSITIVE NON-T, N OR L CA CURRENT COMPONENT OF DORSAL RAPHE NEURONS.

((N.J. Penington and A.P. Fox)) SUNY, Health Science Center Brooklyn, New York & Univ. Chicago, Dept. Pharm./ Phys., Chicago IL. 60637. (Spon. by A.B. Harkins)

Using nimodipine or ω-Conotoxin GVIA (ω-CgTx) to selectively block N- and L-type Ca currents respectively, we previously reported that raphe neurons possess T-, N-, and L-type Ca currents. On average about 45% of the whole-cell I_{Ca} was insensitive to blockade and may represent a new component of Ca current. We have examined the effects of ω-AGA-IVA and ω-Conotoxin MVIIC (ω-MVIIC) on raphe neuron Ca currents. ω-MVIIC (1 μM) blocked 74% of I_{Ca} (N=5). ω-MVIIC blocked 30% of the I_{Ca} remaining after exposing cells to ω-CgTx (1 μM), nimodipine (1 μM) and ω-AGA-IVA (100 nM). ω-AGA-IVA produced a 0-10% reduction in peak I_{Ca}, which suggests that raphe neurons have few P-type Ca channels. ω-AGA-IVA (N=7) had no effect on I_{Ca} if the cell was first treated with either ω-MVIIC or ω-CgTx which implies that the small effect observed was not selective for P-type Ca channels. 5-HT inhibits whole cell I_{Ca} in raphe neurons by activating a 5-HT_{1A} receptor. 5-HT (1 μM) reduces I_{Ca} by 50% and slows activation of the current. In the presence of ω-CgTx (1 μM), nimodipine (1 μM) and ω-AGA-IVA (100 nM), 5-HT still produced ~50% reduction of I_{Ca}, which indicates that 5-HT acts on both blocker-sensitive (N-type Ca channels) and blocker-resistant Ca channels. After treatment with ω-MVIIC, 5-HT was 47% less effective at inhibiting I_{Ca}. The Ca current that was resistant to block is similar to N-type Ca current in that it was blocked by 5-HT, it showed a similar sensitivity to block by Ni^{2+} (50 μM) and it activated and inactivated over the same range of potentials as do N-type channels. Thus, raphe neurons express I_{Ca} that is not sensitive to any known organic Ca channel antagonist, but is difficult to distinguish from N-type Ca current.

M-AM-H2

EVIDENCE FOR P-TYPE CALCIUM CHANNELS AT THE MAMMALIAN NEUROMUSCULAR JUNCTION: A STUDY WITH ω-AGATOXIN IVA, ω-CONOTOXIN GVIA, NIMODIPINE AND AUTOANTIBODIES.

((Yong I. Kim, J.M. Longacher and M.P. Viglione)). *Departments of Biomedical Engineering and Neurology, University of Virginia School of Medicine, Charlottesville, VA 22908.*

Calcium channels at the mammalian neuromuscular junction (NMJ) are sensitive to funnel-web spider toxin FTX (Uchitel *et al. Proc. Natl. Acad. Sci.* **89**: 3330, 1992) and a synthetic peptide toxin, ω-agatoxin IVA (ω-AgTx) (Kim *et al. Mol. Biol. Cell* 4 [suppl]: 428a, 1993). We further characterized and compared the prejunctional action of ω-AgTx, ω-conotoxin GVIA (ω-CgTx) and nimodipine at the mouse NMJ. ω-AgTx did not alter the postjunctional sensitivity to ACh or the resting intraterminal $[Ca^{2+}]_i$ as neither the amplitude nor the frequency (*f*) of spontaneous MEPPs was significantly affected. ω-AgTx specifically reduced quantal content (*m*) of the evoked EPPs, measured from muscles bathed in 1.6 mM Ca^{2+}/10 mM Mg^{2+} using the direct, indirect variance and failure methods. ω-AgTx (1, 5, 10, 20, 40, and 100 nM) reduced *m* in a dose-dependent manner with a K_d of 19.4 nM. The effect saturated at 100 nM, which blocked *m* by >95% (n=27 fibers). Consistent with the voltage-dependent blockade of presynaptic Ca^{2+} channels, the toxin effectively antagonized the stimulatory action of high $[K^+]_o$ on MEPPs. In the control condition, 17.5 mM $[K^+]_o$ produced a 105-fold increase (n=41) in *f*. This effect was diminished by 77% by 40 nM ω-AgTx (n=39). In contrast, ω-CgTx and nimodipine (0.1, 1 and 10 μM) failed to modify synaptic transmission, causing no detectable change in *m* or *f*. Thus, P-type Ca^{2+} channels are the predominant form of Ca^{2+} channels mediating exocytosis at the mammalian NMJ. The Lambert-Eaton syndrome (LES) antibodies likewise reduce *m* at the mouse NMJ, suggesting that the presynaptic target of the LES IgG is the P-type Ca^{2+} channel (Supported by NIH grant NS18607 and the Muscular Dystrophy Association).

M-AM-H3

SPATIAL DISTRIBUTION OF CALCIUM CHANNELS IN NEURONS OF THE SQUID GIANT FIBER LOBE.

((MB McFarlane* and WF Gilly)) Departments of Molecular & Cellular Physiology* and Biology, Stanford University, Hopkins Marine Station, Pacific Grove, CA 93950.

Cultured squid giant fiber lobe (GFL) neurons have been employed previously in studies of sodium channel distribution (Horrigan, et al., 1990), where sodium channels are not expressed in cell bodies *in vivo* and are preferentially targeted to the giant axon. This polarity is maintained *in vitro*, as GFL cell Na channel expression occurs only in growing end-bulbs of axons. We have utilized this *in vitro* system to study the spatial distribution of Ca channels. Two types of Ca channels are present in cell bodies of GFL neurons, and are distinguishable primarily by closing (tail current) kinetics, with a fast-deactivating (FD) channel closing approximately 10 times more rapidly than a slow one (SD) at -80 mV (Llano & Bookman, 1986). FD currents represent 70-90% of the total G_{Ca}, and this proportion remains relatively constant over 0-7 days *in vitro* (DIV). FD currents are the major current type in the developing axon bulb and account for the majority of total G_{Ca} at peak voltage; in several axon bulbs SD currents were barely detectable. Data from acutely dissociated axon bulbs (0 DIV) demonstrate that FD channels are present in similar proportions to cultured axon bulbs (2-7 DIV). The presence of FD channels in axon bulbs indicates a major difference between bulbar membranes and giant axon membranes *in vivo*, where FD channels appear to be absent (DiPolo, et al., 1983). This differs from the distribution of Na channels, where axon bulb Na channel density approaches that of giant axon. We posulate that FD channels are normally found in the presynaptic motor terminals of the giant axon *in vivo*.

M-AM-H4

NO CURRENT-DEPENDENT INACTIVATION OF CLONED N-TYPE Ca CHANNELS TRANSIENTLY EXPRESSED IN MAMMALIAN CELLS

((D.L. Brody, S.J. Dubel, T.P. Snutch, and D.T. Yue)) Johns Hopkins Sch. Med., Baltimore, MD 21205

N-type Ca channels conduct much of the Ca^{2+} influx mediating neurotransmitter release from many presynaptic terminals (Hong *et al*, Neurosci **48**:727). An important form of negative feedback would be Ca^{2+}-entry or current-dependent inactivation of these channels, the existence of which is suggested preliminarily for N-type current in DRG neurons (Cox & Dunlap, Biophys J **64**:A320). The issue remains uncertain, however, because multiple subtypes of Ca channels co-exist in neurons, including the L-type homolog which unequivocally demonstrates Ca^{2+}-dependent inactivation. Here we ask whether Ca^{2+}-dependent inactivation is present in a pure population of N-type Ca channels transiently expressed in HEK293 cells by co-transfection of CMV-based expression vectors carrying the rat brain Ca channel α_1 (rbB-1, Dubel *et al*, PNAS **89**:5058) and β (Pragnell *et al*, FEBS 2:253) subunits. Transfected cells yield macroscopic currents whose activation and inactivation kinetics do not differ appreciably when Ca^{2+} substitutes for Ba^{2+} (10 mM) as charge carrier (A). Moreover, the rate of inactivation increases monotonically with voltage, regardless of charge carrier. These two macroscopic properties already argue against appreciable Ca^{2+}-dependent or current-dependent inactivation. At the single-channel level, there is no consistent difference in unitary gating or decay of ensemble average current whether 110 mM Ba^{2+} or Ca^{2+} carries current (B). Conditional open probability analysis of elementary events provides no clear evidence for "gating plasticity," a single-channel hallmark of Ca^{2+}-dependent inactivation (Yue *et al*, Science **250**:1735). Hence, at least this form of N-type channel shows no current-dependent inactivation as observed in native as well as recombinant L-type Ca channels (de Leon *et al.*, this meeting).

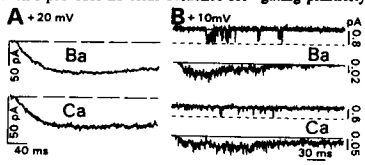

M-AM-H5

IDENTIFICATION OF α_1-β SUBUNIT INTERACTION SITES: IMPLICATION FOR THE MECHANISM OF ß INDUCED STIMULATION OF Ca^{2+} CURRENT. ((M. De Waard, M. Pragnell* and K.P. Campbell)) Howard Hughes Medical Institute, Neuroscience Program* and Dept. of Physiology and Biophysics, University of Iowa College of Medicine, Iowa City, IA 52242.

The purified skeletal muscle dihydropyridine receptor and brain ω-conotoxin receptors both consist of four subunits (α_1, β, α_2 and, γ or 95 kDa). The α_1 subunit is the principle transmembrane subunit that contains the pore of the ion channel and encodes the main functional properties of the complex. So far all ß subunits coexpressed with α_1 subunits stimulate the peak amplitude and modify the voltage-dependence and kinetics of Ca^{2+} currents. The cDNAs encoding β subunits from four genes have been cloned. Sequence comparisons of these subunits show a high degree of homology within two domains. We have investigated the structural basis for the Ca^{2+} current stimulation by β subunits and have identified a conserved region that accounts for this function. Mutational analysis of this region is now underway to further characterize the functional contribution of the ß subunit. Protein overlay experiments will be performed to determine whether the ß subunit site interacts with the recently identified α_1 subunit motif (Pragnell M. et al., Society for Neuroscience Abstract 19, p.1755, abst. 721-14, 1993).

M-AM-H6

HETEROLOGOUS EXPRESSION OF NEURONAL BI CALCIUM CHANNELS IN DYSGENIC SKELETAL MUSCLE.
((B.A. Adams*, T. Tanabe, Y. Mori and K.G. Beam)) *Department of Physiology & Biophysics, University of Iowa, Iowa City, IA 52242-1109.

Expression plasmids carrying cDNA encoding the neuronal BI calcium channel were microinjected into the nuclei of dysgenic myotubes grown in primary culture. Ionic calcium channel currents and intramembrane charge movements were recorded using the whole-cell patch-clamp technique. Injected myotubes expressed high densities (~30 pA/pF) of a calcium current that was not blocked by the dihydropyridine antagonist (+)-PN 200-110. At 20-23 °C, peak currents activated with a time constant (τ_a) of ~2 ms and inactivated with a time constant (τ_h) of ~120 ms. τ_h was not increased by substituting equimolar barium for calcium as charge carrier, indicating that BI channels expressed in dysgenic myotubes do not undergo calcium-dependent inactivation. The maximum density of intramembrane charge movement produced by expression of BI channels was very low compared with the maximum density of the expressed calcium conductance, suggesting that BI channels open with high probability. Injected myotubes failed to contract in response to electrical stimulation via an extracellular pipette; thus, excitation-contraction coupling was not restored by expression of neuronal BI calcium channels. Supported by NIH grant NS 24444 to K.G. Beam.

M-AM-H7

TWO PARALLEL PATHWAYS THAT COUPLE SOMATOSTATIN RECEPTORS TO CALCIUM CHANNEL INHIBITION.
((S.D. Meriney[1], D.B. Gray[2],and G.R. Pilar[2])). [1]Dept. of Behav. Neurosci., Univ. of Pittsburgh, Pittsburgh, PA 15260. [2]Dept. of Physiol. & Neurobiol., Univ. of Connecticut, Storrs, CT 06269.

Using the perforated patch-clamp technique, somatostatin-mediated inhibition of Ca^{2+} current in ciliary ganglion neurons could be consistently observed following repetitive application and strikingly, was not characterized by a second phase of slow Ca^{2+} current activation. Slow Ca^{2+} current activation following membrane-delimited inhibition by neuropeptides has been observed using whole-cell recording. In perforated patch recordings, when cGMP-dependent protein kinase (cGMP-PK) was selectively inhibited by Rp-8-pCPT-cGMPs, somatostatin-induced inhibition of Ca^{2+} channels resembled that observed with traditional whole-cell techniques: an effect that rapidly desensitizes and is characterized by a slowing of activation kinetics. A selective activator of cGMP-PK (Sp-8-Br-cGMPs) could mimic the effect of somatostatin only in cells studied with the perforated patch clamp technique. 8-Br-cAMP was without effect. In intact cells, somatostatin receptors trigger both a membrane-delimited and soluble signal transduction cascade (through cGMP-PK) that leads to a sustained inhibition of neuronal Ca^{2+} channels. Supported by NIH NS10338, NSF IBN-9213204, and visiting scholar support from UCONN.

M-AM-H8

ENHANCEMENT OF CALCIUM CHANNEL ACTIVITY IN HIPPOCAMPAL NEURONS BY MEMBRANE-PERMEABLE ANALOGS OF cAMP. ((Ege T. Kavalali and Mark R. Plummer)) Dept. of Biological Sciences, Nelson Lab, Busch Campus, Rutgers University, Piscataway, NJ 08855-1059

Cell-attached single-channel recordings from hippocampal neurons have revealed a novel dihydropyridine-sensitive calcium channel that shows a form of voltage-dependent potentiation characterized by bursts of re-openings following conditioning depolarizing voltage pulses (Lp channel). To determine whether Lp potentiation can be modulated, we have examined the effects of PKA activators. When compared to controls (sweeps on left; time period analyzed indicated by dashed lines) recordings from patches with Lp channels in the presence of 1 mM 8-CPT-cAMP (sweeps on right) showed a significant increase in average re-opening probability (0.006 ± 0.0001 vs. 0.012 ± 0.002; $p < 0.01$; Student's t-test, two-tailed) at a -40 mV test potential following 320 msec prepulses to +40 mV. This was due to increased numbers of openings (means: 2.3 ± 0.27 vs. 6.89 ± 0.64) rather than increased mean open time. We are currently investigating the effects of other kinase activators and selective protein kinase inhibitors on this enhanced activity.

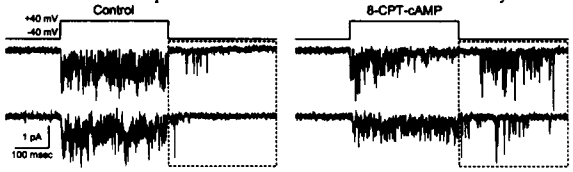

M-AM-H9

CA CHANNELS OPEN AT NEGATIVE POTENTIAL FOLLOWING ACTION POTENTIAL WAVE.
((A. Galli, A. Ferroni and M. Mazzanti))Dept. of Physiology and Biochemistry, Milano, I-20133, ITALY.

Neuronal cell firing is crutial to nerve-nerve communication. The ability to produce consecutive action potentials is related to the activation of inward currents after each upstroke. If fast Na current is indeed responsible for the overshoot, it is still unclear which current drives membrane voltage to the Na threshold. In the present study we present evidence that in adult rat sensory neurons a dihydropyridine sensitive Ca channel exists in addition to the well characterize L-type or high-threshold Ca channel. During stimulated action potential trains, L-type Ca channels open during the excitation wave, whereas the other dihydropyridine sensitive Ca channel was observed mainly between action potentials. This second Ca pathway shows remarkably long openings at negative potentials after positive prepulses. The nerve action potential works as a physiological facilitation voltage step. Therefore it induces Ca entry not only during firing, but also during the latent period between action potential.

M-AM-H10

TAIL CURRENTS THROUGH R-TYPE CALCIUM CHANNELS IN CHROMAFFIN CELLS ((Andrea Fleig & Reinhold Penner)) *Max-Planck-Inst. for Biophysical Chemistry, 37077 Göttingen, Germany.*

Based on their voltage-dependence, kinetics, and pharmacological profile, at least four families of Ca channels have been characterized (L-, N-, T-, and P-type calcium channels). These are activated by membrane depolarization and conduct Ca^{2+} ions according to the electrochemical driving force, yielding a bell-shaped current-voltage relationship with a peak around 0 to +20 mV. We report the presence of a novel type of voltage-dependent Ca channel in bovine chromaffin cells which, under physiological conditions, does not carry detectable inward current during depolarizations but produces large tail currents when returning to negative voltages. Since these tail currents flow upon repolarization and display inward rectification, we designate the corresponding Ca channels as R-type. Similar to L-type Ca channels, tail Ca currents have a high threshold for activation (half-maximal activation at +20 mV). Tail currents may be carried by Ca^{2+} or Ba^{2+} ions, but unlike L-type channels, R-type channels are highly resistant to Cd^{2+} block (IC_{50} = 1 mM). Tail currents through R-type channels are enhanced by Bay K 8644 (5μM), but resistant to dihydropyridine block (5 μM nifedipine). These channels may carry a significant amount of Ca^{2+} during short action potentials to support transmitter release.